AD_____

Award Number: DAMD17-01-1-0820

TITLE: Effects of Low Level Radiation Exposure on Neurogenesis
        and Cognitive Function: Mechanisms and Prevention

PRINCIPAL INVESTIGATOR: John R. Fike, Ph.D.

CONTRACTING ORGANIZATION: University of California, San Francisco
                           San Francisco, California 94143-0962

REPORT DATE: September 2003

TYPE OF REPORT: Annual

PREPARED FOR: U.S. Army Medical Research and Materiel Command
               Fort Detrick, Maryland 21702-5012

DISTRIBUTION STATEMENT: Approved for Public Release;
                        Distribution Unlimited

The views, opinions and/or findings contained in this report are
those of the author(s) and should not be construed as an official
Department of the Army position, policy or decision unless so
designated by other documentation.

REPORT DOCUMENTATION PAGE

1. AGENCY USE ONLY (Leave blank)	2. REPORT DATE Septmeber 2003	3. REPORT TYPE AND DATES COVERED Annual (1 Aug 2002 – 1 Aug 2003)

4. TITLE AND SUBTITLE
Effect of Low Level Radiation Exposure on Neurogenesis and Cognitive Function: Mechanisms and Prevention

5. FUNDING NUMBERS
DAMD17-01-1-0820

6. AUTHOR(S)
John R. Fike, Ph.D.

7. PERFORMING ORGANIZATION NAME(S) AND ADDRESS(ES)
University of California, San Francisco
San Francisco, California 94143-0962

E-Mail: jfike@itsa.ucsf.edu

8. PERFORMING ORGANIZATION REPORT NUMBER

9. SPONSORING / MONITORING AGENCY NAME(S) AND ADDRESS(ES)
U.S. Army Medical Research and Materiel Command
Fort Detrick, Maryland 21702-5012

10. SPONSORING / MONITORING AGENCY REPORT NUMBER

11. SUPPLEMENTARY NOTES

20040116 019

12a. DISTRIBUTION / AVAILABILITY STATEMENT
Approved for Public Release; Distribution Unlimited

12b. DISTRIBUTION CODE

13. ABSTRACT (Maximum 200 Words)

Studies were carried out to investigate that radiation response of neural precursor cells in vitro and in vivo, to determine the role of reactive oxygen species (ROS) in the reactions of those cells, and to determine if antioxidant treatment could modify those responses. Our data show that proliferating precursor cells and their progeny are extremely sensitive to low/moderate x-ray doses (2-10 Gy), and the ROS play a major role in the sensitivity on these cells and any act in concert with p53 and cell cycle-dependent processes. In addition, conditions of reduced cell density, such as that seen after radiation exposure of the denate subgranular zone, are associated with increased ROS, which may stimulate proliferation in surviving cells. Modulating ROS using antioxidant compounds may provide a means to control proliferation in damaged cells allowing for repair and recovery after radiation injury. We have begun to address specific mechanistic factors that are not only associated with oxidative processes, but that may provide additional targets for interventional treatment. The ability to ameliorate the radiation effects on neural precursor cells may provide a potential protective strategy for individual exposed to unplanned exposure to low/moderate doses of irradiation.

14. SUBJECT TERMS No Subject Terms.			15. NUMBER OF PAGES 34
			16. PRICE CODE

17. SECURITY CLASSIFICATION OF REPORT Unclassified	18. SECURITY CLASSIFICATION OF THIS PAGE Unclassified	19. SECURITY CLASSIFICATION OF ABSTRACT Unclassified	20. LIMITATION OF ABSTRACT Unlimited

Table of Contents

INTRODUCTION: Uncontrolled radiation exposure from a nuclear battlefield will lead to a wide range of delivered doses and subsequent tissue/body effects. However, such exposure does not have to be lethal to have significant consequences. The depletion of stem/precursor cells, for instance could lead to prolonged effects in some tissues, particularly if those cells have limited regenerative potential. Because of the role of hippocampal neuronal precursor cells in the development and maintenance of memory, we hypothesize that these cells are critical targets in the radiation-induced impairment of cognitive function. We contend that radiation-induced loss of these cells will decrease neurogenesis and lead to cognitive changes. We hypothesize that such effects are mediated through oxidative stress, and that by reducing oxidative injury we can ameliorate radiation-induced cognitive impairment. This research project involves a series of *in vitro* and *in vivo* laboratory studies to assess the effects of ionizing irradiation on neural precursor cells, neurogenesis and cognitive function. The experiments will assess the role of oxidative processes in the development of radiation injury and determine the efficacy of antioxidant strategies in reducing that injury.

BODY: This research project consists of 3 objectives which are: 1) using low to moderate radiation doses to simulate a battlefield exposure, quantify the effects of x-rays on dentate subgranular zone (SGZ) neurogenesis, and determine if such exposure is associated with the development of cognitive impairment; 2) using biochemical measures of oxidative stress determine the effects of x-rays on neural precursor cells in culture and test the ability of antioxidant compounds to reduce those effects; and 3) determine if antioxidant treatment during exposure to x-rays will ameliorate radiation-induced effects on neural precursor cells, neurogenesis and subsequent cognitive function.

The Statement of Work for the second year of funding listed 2 primary goals: 1) complete the histologic analyses of tissues irradiated the first year and complete the *in vitro* studies assessing the ability of antioxidant compounds to reduce radiation injury to neural precursor cells in culture; 2) initiate *in vivo* studies designed to determine if antioxidant agents will reduce early radiation-induced changes in precursor cell proliferation. Our findings to date are summarized below.

In Vitro Studies:

In the first year of funding we elucidated a number of important characteristics of neural precursor cells in culture. Briefly, these cells are very sensitive to low doses of irradiation, undergoing apoptosis within 12 hours of exposure. The apoptotic changes are associated in time and radiation dose with elevations in reactive oxygen species (ROS) indicating that oxidative damage plays an important role in the acute and chronic radiation response of neural precursors. We also were able to provide preliminary evidence that ROS and apoptosis could be modulated using a superoxide dismutase (SOD) mimetic compound, Euk-134. In order to identify targets or processes that may be involved in ROS-mediated effects within neural precursor cells we have expanded our studies of the biology of these cells and addressed factors that affect their radiation responsiveness. Further, we completed a number of studies assessing the effectiveness of antioxidant compounds. These data, which are summarized below have been and currently are being used to direct our *in vivo* studies.

General methods:
Neural precursor cells were derived from the rat hippocampus, as described previously (1). These cells, which exhibited routine doubling times of 20 – 28 hrs, were maintained in exponential growth and passaged twice weekly. Cells were grown in the presence of serum-free DMEM/F12 (1:1) containing N2 supplement and 20 ng/ml of fibroblast growth factor-2 (FGF-2). All cultures were grown on polyornithine/laminin coated plasticware and re-fed every other day using a ratio of 3:1 new:conditioned medium.

The detection of intracellular ROS was based on the ability of cells to oxidize a fluorogenic dye to its corresponding fluorescent analog. Exponentially growing cultures were treated for 1h at 37°C with 5 µM of the ROS sensitive dye 5-(and-6)-chloromethyl-2',7'-dichlorodihydrofluorescein diacetate (CM-H$_2$DCFDA). Immediately following dye incubation, cells were harvested and

subjected to fluorescent automated cell sorting (FACS). For each post-irradiation time point, ROS measurements for irradiated and sham-irradiated control cultures were performed in parallel. All measurements were performed in duplicate or triplicate and were derived from independently irradiated cultures of cells.

Apoptosis assays were performed using FACS analysis, and were done in parallel with measurements of ROS. To normalize experimental conditions for each of the endpoints assayed, cells to be assayed for apoptosis were passaged and re-fed at the same time as those flasks used for the ROS measurements. At each post-irradiation time, cells were harvested, rinsed in PBS, and incubated for 20 min at ambient temperature in limiting volumes (~0.2-0.5 ml) of binding buffer containing FITC-conjugated annexin V. Cells suspensions were brought to 0.5-1.0 x 10^{6}cells/ml in PBS and immediately subjected to FACS analysis. As with ROS measurements, apoptotic assays were performed in duplicate or triplicate and derived from independently irradiated cultures of cells. FACS data was also analyzed using the ModFit LT^{TM} program to estimate the percentage of apoptotic cells from cell cycle histograms.

Cell cycle effects:

Given that proliferating precursor cells *in vivo* and *in vitro* are extremely sensitive to a radiation-induced apoptotic cell death (Year 1 Progress Report, and Refs. 2, 3), we wanted to determine the relationship between the apoptosis induced by low doses of irradiation and the inhibition of cell cycle progression. These studies are significant because perturbations in cell cycle progression could severely impact the capability of stem/precursor cell pools to properly respond to and repopulate regions of the CNS incurring radiation damage. Exponentially growing cultures of neural precursor cells were either sham irradiated or exposed to 5 Gy and at various times after irradiation (6, 12, 18, 24, and 48 h) fixed in 70% ethanol and stored at −20°C. On the day of assay, samples were resuspended for 1 h at ambient temperature in isotonic phosphate buffered saline (PBS) supplemented with RNAse (50 U/ml) and propidium iodide (PI, 10 μg/ml). Subsequently, cells were assayed for DNA content by FACS analysis of PI fluorescence. Raw data were gated to eliminate debris and doublets, and to calculate the distribution of cells throughout the cell cycle. A minimum of 30,000 cells were analyzed at each time point using the ModFit LT^{TM} analysis software. Reverse chi square values were routinely under 5 indicating that the cell cycle data were within the parameters of the Mod-Fit algorithm.

Cell cycle analyses of irradiated precursor cells confirmed the presence of functional radiation-induced checkpoints, particularly in G2/M (**Fig. 1**). The peak of G2/M arrest coincided with the time of maximal apoptosis and maximal generation of ROS. The activation of cell cycle checkpoints is consistent with a DNA damage response expected for cells containing a functional p53 protein (4). To substantiate that p53 played a role in the
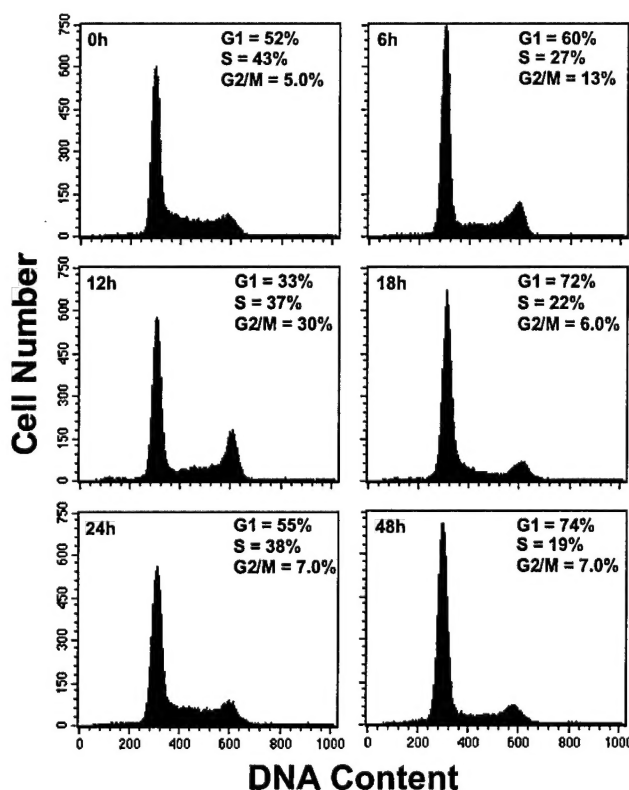

Fig. 1: Activation of cell cycle checkpoints after x-irradiation. Histograms illustrate functional G2/M and G1/S checkpoints as evidenced by the pronounced buildup of cells in the G2/M (12 hr) and G1 (18 h) cell cycle compartments, respectively

observed radiation response of precursor cells, we irradiated cultures with 5 Gy and analyzed for p53-dependent increases in protein levels and phosphorylation by western blot. Our results showed that p53 levels increased with time after irradiation and that these elevations were accompanied by an increase in p21 levels and p53 phosphorylation at serine 15 (**Fig. 2**). These results provide evidence that p53 has a role in the radioresponse of neural precursor cells.

Data demonstrating that p53 might regulate the behavior of neural precursor cells to irradiation is potentially significant to this proposal for several reasons. First it is well established that p53 acts to safeguard an organism against the accumulation of cells harboring potentially deleterious genetic
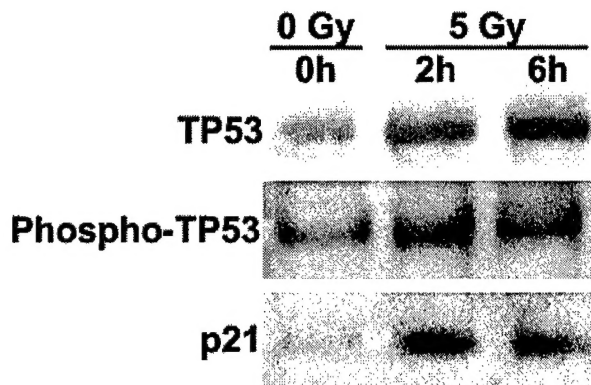

Fig. 2: X-rays activate the p53 (TP53) pathway. Compared to controls p53 protein levels increases ~ 2 and 4-fold at 2 and 6 hr after irradiation. Increases in p53 were associated with an increase in ser15 phospho-p53 and p21 levels. All sample loading was normalized to protein content.

changes accumulated over time or in response to an acute stress (such as an unanticipated exposure to radiation). To accomplish this, p53 acts to slow cell cycle progression in the presence of DNA damage, thereby promoting DNA repair to minimize the impact of stress upon the cell and organism. Second, p53 regulates apoptosis, which is believed to provide a means for removing damaged cells. However, signaling events from neighboring cells and the surrounding environment have also been shown to activate p53. This has the potential to promote the elimination of otherwise normal and undamaged cells in the hippocampus. The inability to properly regulate the p53-dependent apoptotic response to irradiation, may lead to dysfunctional cells integrating into higher tissues that may compromise physiology (e.g. cognitive function). Third and perhaps most important, p53 regulates the expression of redox sensitive genes that act in multiple pathways (5). These pathways regulate the level of antioxidants and pro-oxidants in the cell and surrounding microenvironment that can greatly impact the inherent radiation sensitivity of cells. Thus, the link between p53 and ROS provides a logical mechanism for regulating the survival of neural precursor cells exposed to radiation. Our studies may also provide the rationale for genetically screening individuals for p53 mutations that might predispose them to additional risks associated with radiation exposure.

Density Effects: The redox status of cells is critical to the regulation of multiple damage-responsive pathways, such as that mediated through p53. Redox status is intimately dependent on the level of ROS, and ROS have multiple roles in mediating and affecting cellular physiology. At high levels, ROS can damage cellular molecules and activate stress-responsive pathways in cells. However, at relatively low levels, ROS can act to signal metabolic change or environmental stress. ROS can directly or indirectly activate signaling pathways and can operate intra-or extracellularly. ROS are believed to provide one of the many cues that regulate proliferation and survival in response to damage (6), and the presence of extracellular antioxidants indicates that cells have evolved mechanisms to specifically regulate exogenous ROS (7, 8).

Because a predominant effect of irradiation *in vivo* is a significant reduction in the proliferating precursor cells and their progeny, immature neurons (see below), we were interested in determining how the loss of a significant proportion of a given cell population might affect redox state in the surviving fraction. Consequently, we have developed an *in vitro* model to simulate the situation of neural precursor cell depletion observed after irradiation. Our model involves a simple yet elegant manipulation of the cultured cell density.

To determine redox state as a function of cell density, we plated un-irradiated neural precursor cells at low ($\sim 10^4$ cells/cm^2) to high ($\sim 3 \times 10^5$ cells/cm^2) density. We then assessed ROS and antioxidant levels, mitochondrial function, and cellular proliferation. Low density cultures exhibited significantly higher levels of ROS than high density cultures. Interestingly, this trend was not observed in transformed cell lines, and absolute levels of ROS were generally 3-5 fold higher in the neural precursor cells (**Fig. 3**). ROS levels at low densities were found to coincide with

mitochondrial dysfunction (**Fig. 4**), implicating the mitochondria as the source of elevated ROS. It was also observed that higher levels of ROS were associated with elevated proliferation as determined by cell doubling time and S-phase fractions (**Fig. 5**). In addition, the transition to higher cell densities was accompanied by an increase in cellular antioxidants (e.g. MnSOD) (**Fig. 6**); this may underlie the reduced ROS observed at high cell densities. These density dependent changes were reversed with the antioxidant α-lipoic acid (**Fig. 7**). These data show that neural precursor cells are predisposed to redox sensitive changes that are responsive to density dependent cues that regulate ROS and antioxidant levels to control cellular proliferation. *In vivo*, a similar situation can be expected after CNS damage, where radiation-induced depletion of precursor cell numbers would stimulate ROS-dependent increases in cellular proliferation; preliminary data shown below substantiates this idea, and validates the applicability of modeling damage-induced depletion of neural cells *in vivo*, through *in vitro* manipulations of culture density.
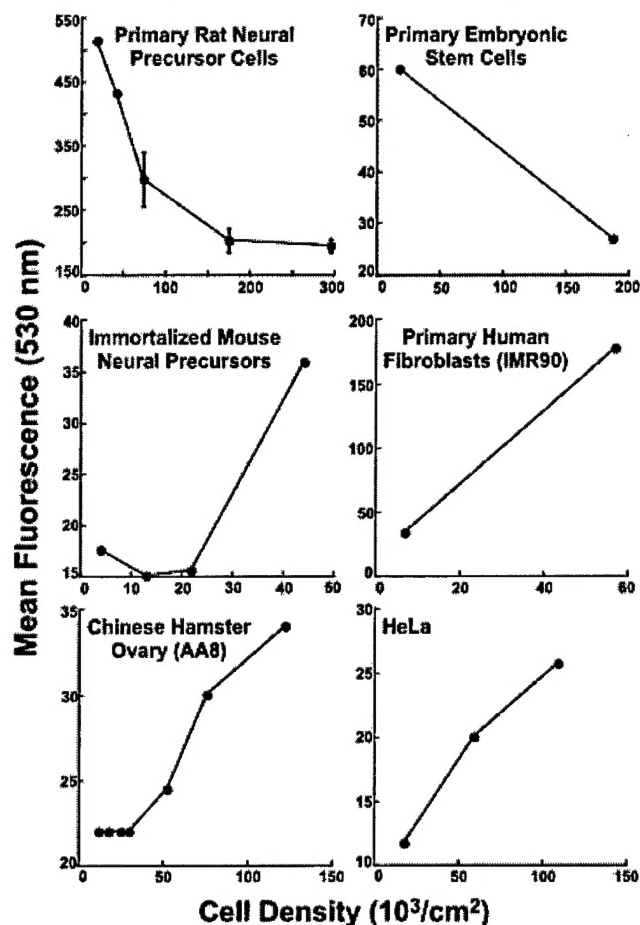

Fig. 3: Cell type and cell density dependent production of reactive oxygen species in various mammalian cells. The ordinate represents relative ROS production
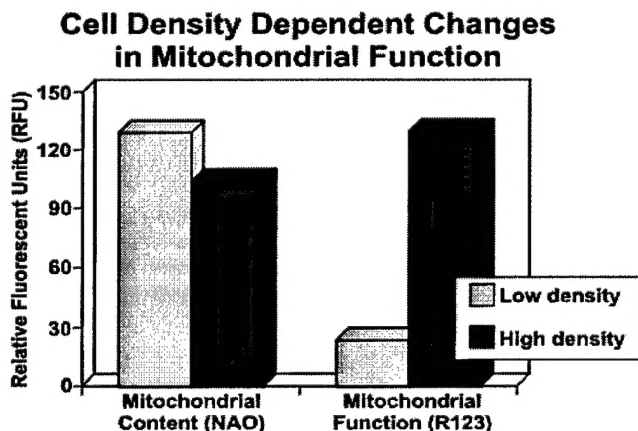

Fig. 4: ROS levels (fluorescent units), which are elevated under conditions of low cell density (Fig. 3) are associated with mitochondrial dysfunction.

Antioxidant treatment:

Clearly, the normal behavior and damage (radiation) response of neural precursor cells in culture is mediated in part through ROS. Furthermore the changes observed *in vitro* mirror similar changes detected using our *in vivo* model of radiation injury to the hippocampal dentate gyrus (see below). Based on cell culture data as well as preliminary studies done the first year of funding, we wanted to determine if specific measures of radiation-induced oxidative damage could be reduced by using antioxidant treatments. Preliminary experiments using SOD mimetic compounds provided by Dr. Susan Doctrow were initially promising, but have recently been hindered by side reactivities inherent to many of these Euk compounds (i.e. Euk-134, 161, 163, 172, 189) (9). Briefly, each Euk analog converts superoxide to hydrogen peroxide and hydrogen peroxide to water and oxygen. The first reaction is relatively insensitive to small structural changes while the second reaction is quite structurally dependent. Furthermore, after the first reaction is complete each Euk compound has a competing peroxidase activity that can oxidize (not scavenge) other cellular molecules. This is evidenced by the increased fluorescence observed using redox-sensitive dyes in conjunction with the Euk analogs. Using these dyes we have already demonstrated
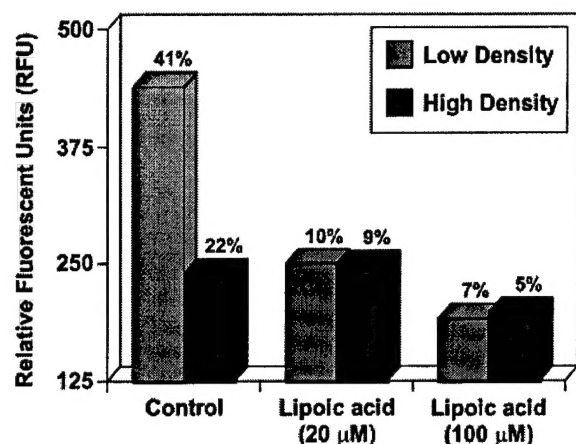
Fig. 5: Density-dependent ROS (fluorescent units) are associated with elevated proliferation. The S-phase fractions of each population are indicated by the percentage numbers at the top of each bar. Lipoic acid eliminates this effect.
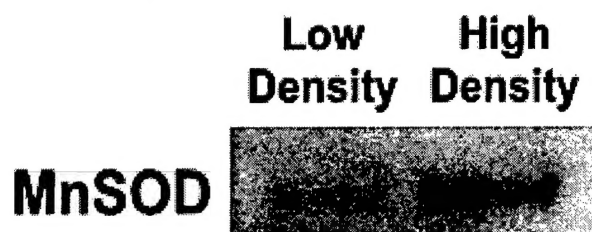
that irradiation leads to increased ROS (not shown). Addition of Euk analogs potentiates this increase by oxidizing the redox-sensitive dye itself. Further work is currently underway to pinpoint the appropriate treatment regime *in vitro* that might minimize peroxidase activity while maximizing scavenging activities. These developments may, however, limit the broad based utility of these compounds as antioxidants. In part due to these results, we have also begun studies using lipoic acid as an antioxidant. Preliminary *in vitro* data has indicated that this compound may provide a better means for reducing the impact of ROS after radiation damage.

Fig. 6: MnSod is increased in cells plated at high density.

Fig. 7: Density dependent changes in ROS (fluorescent units) are reversed with the antioxidant compound α-lipoic acid.

In Vivo Studies

In the first year of funding we were able to document the acute and longer term effects of low to moderate doses of x-rays on the neural precursor cell population in the dentate SGZ of mice. The results from those studies showed that: 1) proliferating precursor cells and their progeny, immature neurons, are extremely sensitive to irradiation, undergoing an apoptotic cell death ~ 12 hr after exposure; 2) acute changes in those cells were associated with altered neurogenesis, i.e. the production of new neurons; and 3) altered neurogenesis was associated with later developing cognitive impairments. The quantification of neurogenesis was accomplished using confocal microscopy, a methodology developed in our lab after the submission of the original grant proposal. This methodology provided us a means to quantify not only new neuron production but also the production of astrocytes and oligodendrocytes. We also were able to show, using qualitative immunohistochemistry, that oxidative stress was involved in the changes we observed in the SGZ. In the current funding year we expanded on those studies and have begun investigation of antioxidant treatment to ameliorate these adverse effect of irradiation. These studies were based on, and parallel, many of the *in vitro* investigations summarized above. The results of our ongoing studies are shown below.

General Methods:
Young adult male C57BL wild type (WT) or p53 knock out (KO) mice were used. Anesthesia was required for irradiation and perfusion procedures; intraperitoneal (i.p.) injections of ketamine hydrochloride (65 mg/kg) and medetomidine (0.5 mg/kg) were used. Whole brain irradiation was done as previously described (3), and dose rate was about 175 cGy/min. At specified times after

exposure, animals were anesthetized and perfused with 10 % buffered formalin using parameters previously described (3). After fixation, brains were processed for immunohistochemistry using paraffin embedding; a standardized counting region and protocol were used when quantifying cells in paraffin embedded tissues (3). Quantification was made of all positively-labeled cells within the dentate SGZ of the superior and inferior blades of the dentate gyrus; both hemispheres were counted for each animal. The total number of positively-labeled cells was determined by summing the values from all 3 tissue sections from a given brain. Proliferating cells were detected using an antibody against Ki-67, a nuclear antigen that is expressed during all proliferative stages of the cell cycle except G_0 (10). Immature neurons were detected using an antibody against Doublecortin (Dcx), a protein required for neuronal migration (11). Numbers of cells exhibiting cell-specific staining were scored blind.

Cell Responses and Neurogenesis:

While the previous progress report showed the effects of a single 10 Gy dose of x-rays on proliferating cells (Ki-67) and immature neurons (Dcx), we now have full dose responses including relatively low doses (**Fig. 8**). A Jonckhere-Terpstra test showed that for both endpoints the dose responses from 2-10 Gy were significant ($P < 0.05$). Because immature neurons generally move into the dentate granule cell layer (GCL) as they differentiate, we quantified the numbers of Dcx-positive cells in the GCL to determine if the sensitivity of immature neurons changed as they moved away

Fig. 8: Numbers of proliferating cells (left) and immature neurons (right) in the dentate SGZ are significantly decreased 48 hr after irradiation. Each bar represents an average of 4 mice; error bars are SEM.

from the SGZ. In the SGZ, the percentage decrease in cell number relative to controls was 41%, 53% and 61% after 2, 5 and 10 Gy. The numbers of Dcx-positive cells in the GCL were decreased about 19.8%, 26% and 52.7% after 2, 5 and 10 Gy respectively. This suggests that as newly born cells migrate further away from the SGZ they become less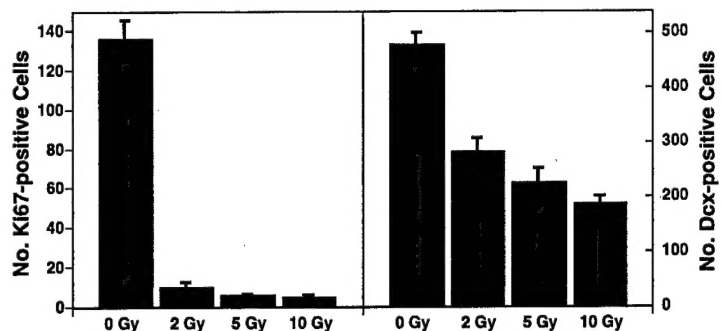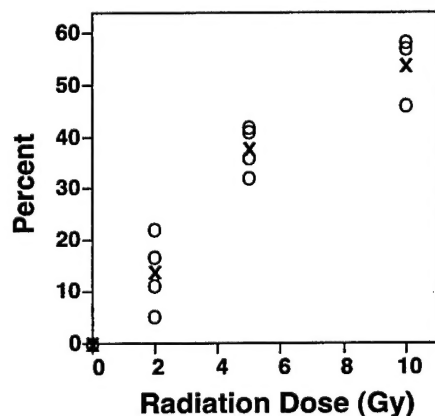 sensitive to irradiation. Whether this represents different environmental factors or simply the fact that the cells are becoming more differentiated is not yet clear.

In the Year 1 Progress Report, and in a recent publication (2), we showed that in the mouse the production of mature neurons was affected in a dose related fashion while the production of new astrocytes and oligodendrocytes were not. We also have shown similar results in the rat, but only after a single dose of 10 Gy (12). In this funding year we also looked at another cell type in the brain, the microglial cell to determine if local inflammation may contribute to our findings. ROS such as superoxide, which is produced by irradiation, has been shown to be an early signal triggering the induction of cytokines from microglia (13). Given the potential role of proinflammatory cytokines in radiation brain injury (14, 15), and the impact of specific cytokines on neurogenesis (16), it is possible that the activation of microglia via ROS or the release of ROS from irradiated microglia, may constitute a critical factor in the radiation-induced inhibition of neuron production. At 48 hr after irradiation, when proliferating cells and immature neurons are significantly reduced, there were no activated microglia

Fig. 9: Two months after irradiation there is a substantial inflammatory response in the dentate SGZ. Proliferating cells were first labeled with the thymidine analog BrdU and 3 weeks later, the relative proportion of cells (percent) staining for BrdU plus the activated microglial marker CD68 were quantified using confocal microscopy. A significant dose-related increase in activated microglia was seen. Each circle represents an individual mouse; each X represents the mean value for a given dose group.

detected in or around the SGZ (2). In contrast, 2 months after irradiation there was a significant dose-related increase in the number of activated microglia (p < 0.001) (**Fig. 9**). While it has not yet been shown what role the increase in activated microglia might play in radiation-induced neurogenesis, this cell type might constitute an effecter for modulating the adverse effects of irradiation in the SGZ. The function/activity of such cells might be ameliorated with antioxidant compounds as proposed in this grant application, or perhaps with anti-inflammatory agents.

The role of p53:

Our *in vitro* studies (above, **Fig. 2**) show that p53 plays a role in the radiation response of neural precursor cells in culture. Given the potential relationship between p53 function and oxidative stress, we wanted to determine if p53 also played a role in the radiation response of precursor cells and immature neurons in the SGZ of mice. Two month old WT and p53 KO mice were anesthetized as described and irradiated with singles doses of 0, 1, 2, 5, and 10 Gy. Forty-eight hours later the mice were perfused and the tissue sections of the dentate gyrus prepared. Proliferating cells and immature neurons were quantified as described above. Before irradiation, the numbers of proliferating cells and immature neurons in p53 KO mice were ~ 20% and 13% higher, respectively, than that seen in WT controls. While relatively few, the number of apoptotic cells in our standardized region of interest (3) was 12 ± 1.1 (mean $\pm$ SEM) in WT and 8 ± 1.7 in KO. After irradiation, the numbers of proliferating cells and immature neurons decreased in a dose-dependent manner in both types of mice (**Fig. 10**). Compared to WT, p53 KO
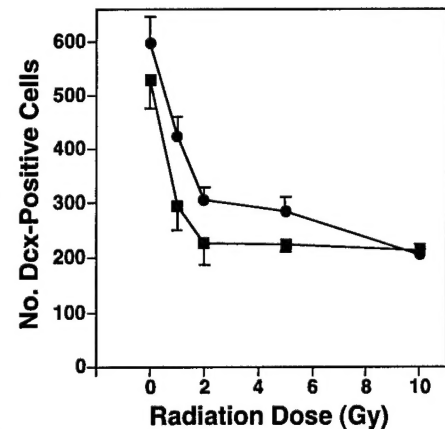

Fig. 10: Dose dependent decreases in the number of immature neurons within the dentate SGZ occur in both wild type (WT, squares) and p53 knock out (KO) mice (circles). Compared to wild type, p53 KO mice showed a statistically significant increase in the number of cells after doses below 10 Gy.

mice showed ~ 20% more proliferating cells; while this trend persisted after irradiation, it was not significantly different at all doses (data not shown). p53 deficient mice did, however, exhibit statistically significant (p<0.05; Wilcoxon-Mann-Whitney) elevations in the number of immature neurons after low doses; there was no difference after the highest dose of 10 Gy (**Fig. 10**). These data support a role for p53 in regulating the radioresponse of neural precursor cells *in vivo*, particularly after lower doses.

Oxidative Stress:

Our general hypothesis is that oxidative stress plays a role in the radiation response of SGZ precursor cells, and our comprehensive *in vitro* data above is clearly supportive. As stated above, we previously reported (Year 1 Progress Report) that 48 hr after irradiation there was a qualitative increase in malondialdehype (MDA) in the dentate SGZ of mice irradiated with 10 Gy. MDA is an endpoint of lipid peroxidation and a reliable marker of oxidative stress. To quantitatively determine if elevated levels of MDA were persistent after irradiation we used a commercial kit that measures MDA in tissue homogenates by colorimetric assay. Hippocampi were dissected from mice irradiated either 2 days or 1 week previously with 10 Gy, and were homogenized. MDA levels in irradiated and nonirradiated brains were determined in triplicate and calibrated against a standard curve generated the day of assay. Compared to unirradiated controls, MDA levels were significantly increased 1 weeks after irradiation (**Fig. 11**).
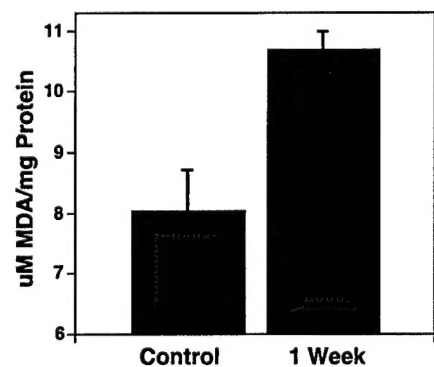

Fig. 11: Lipid peroxidation in the hippocampus of irradiated mice. Tissue was obtained from irradiated (10 Gy) mice and processed for the determination of malonyl dialdehype (MDA). Compared to controls, tissues isolated 1 w eek after irradiation had significantly higher MDA levels. Each bar represents a mean of 6 mice; error bars are SEM.

Antioxidant Treatment:

Considerable *in vitro* and *in vivo* data generated in the first 2 years of funding strongly suggested that ROS play a role in the radiation response of neural precursor cells from the hippocampus. Based on pilot *in vitro* data presented in the Year 1 Progress Report, we initiated a study to determine if the extent of acute cellular changes in the dentate SGZ could be modified using an antioxidant compound. These studies used the superoxide dismutase/catalase mimetic drug EUK-134 at a dose of 30 mg/kg administered intraperitoneally 15 minutes before irradiation. Controls were injected with the solvent which was used to dilute the EUK compound. Tissues were collected either 12hr or 48 hr after irradiation, and numbers of proliferating cells and immature neurons quantified in our standardized region of interest; the results from this study are tabulated below.

	Proliferation Cells (Ki-67)	Immature Neurons (Dcx)
Vehicle Control 12 hr	109 ± 7.0	561 ± 24
Euk 12 hr	131 ± 40	629 ± 38.5
Vehicle + 1 Gy 12 hr	49.5 ± 4.5	371 ± 51
Euk + 1 Gy 12 hr	45.5 ± 7.5	358 ± 77
Vehicle Control 48 hr	106 ± 15	561 ± 24
Euk 48 hr	92 ± 2.0	629 ± 38.5
Vehicle + 1 Gy 48 hr	14 ± 7.0	223 ± 12
Euk + 1 Gy 48 hr	14.5 ± 6.5	233 ± 46

While these results represent a preliminary study using only one administration paradigm, the data show that Euk-134 had no significant effect in terms of reducing radiation injury and in some cases there was actually more cell loss in mice treated with Euk-134 (e.g. Ki-67, 48 hr vehicle vs. 48 hr Euk). While these results may reflect suboptimal treatment parameters, they may also reflect the increased peroxidase activity associated with the Euk compounds (see discussion for *in vitro* studies above).

Based on these preliminary data and the results from our *in vitro* studies we have chosen not to pursue the Euk compounds until the issue of increased ROS is resolved using our *in vitro* model. Instead, and based on favorable *in vitro* results (above) we have initiated animal studies using α-lipoic acid. Those studies have yet to be analyzed.

Density Effects:

We know that low doses of irradiation result in significant reductions is specific cell populations in the dentate SGZ; that information has recently been published (2). Based on the *in vitro* studies described above, we are hypothesizing that the damage-induced loss of cells results in elevated ROS which may play a role in stimulating cell proliferation to repopulate the SGZ. We also know that 1 week following irradiation there are increased MDA levels in the hippocampus indicating an elevated level of oxidative stress. To determine if our *in vitro* findings translate into what may be happening *in vivo* we gave a single dose of 5Gy to mice to deplete proliferating cells and immature neurons, and then 1, 2, 3 7 and 14 days later determined the number of proliferating SGZ precursor cells (**Fig. 12**). The results from this study show that after significant cellular depopulation, cell proliferation is elevated and coincides with increased oxidative stress that was observed 1 week after irradiation. While preliminary, these data do suggest a possible cause and effect relationship linking the regulation of cellular redox state to the repopulation dynamics within the damaged CNS.

In vivo results are consistent with those we obtained *in vitro*, and suggest further that ROS may play a role in critical signaling pathways associated with cell proliferation. Studies are currently underway determining if the anti-oxidant compound α-lipoic acid will impact this proliferative response, and ultimately, neurogenesis and cognitive function. If ROS are stimulants to proliferation *in vivo*, α-lipoic acid may slow down this process and allow reparative processes to occur and spare the depletion of SGZ cells after radiation injury. The results from this study will be reported in the Year 3 Progress Report.
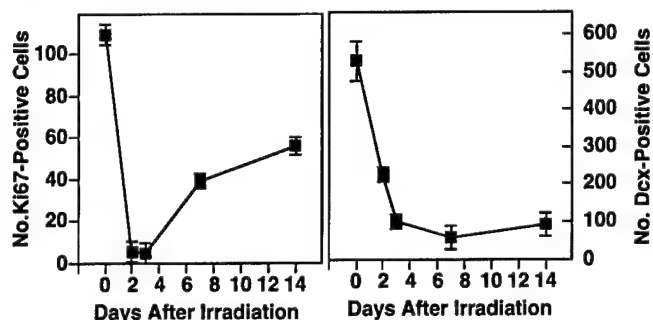

Fig. 12: Changes in numbers of proliferating cells (left) and immature neurons (right) as a function of time after a single dose of 5 Gy. A major loss of proliferating cells 2-3 days after irradiation is followed by a significant increase in proliferation; a concomitant increase in the production of immature neurons is suggested, but is not significant over the time course studied. Each symbol represents a mean of 4 mice; error bars are SEM.

Fractionated Irradiation

One of the stated goals of this project was to irradiate with multiple small doses in order to simulate a battlefield exposure. The studies of the first and part of the second year of funding focused on low to medium single doses in order to establish endpoints, methodology and to determine biological responses in the cells of interest. Once these important factors were determined it was possible to initiate fractionated studies. Because we intended to use up to 5 -10 fractions over 1 -2 weeks, it was necessary to institute shorter term anesthetic protocols to maintain animal health over the treatment period. Therefore we proposed to use short acting isoflurane gas anesthesia because induction and recovery are rapid, generally taking only 1-2 minutes. This facilitated fractionated treatment and was well-tolerated by the animals. Initial studies were done to assess the response of proliferating cells and immature neurons in the dentate SGZ after 5 daily fractions of either 0.5, 1.0 or 1.5 Gy/fraction; tissues were collected 48 hr after the last fraction. Controls included gas anesthesia alone on each of 5 consecutive days. In addition, a separate group of mice received gas anesthesia on 5 consecutive days and during the last anesthesia a single 5 Gy dose was given. This last control allowed us to determine if there was a dose sparing effect when a total dose of 5 Gy was fractionated in 5 equal treatments. The data from this study are
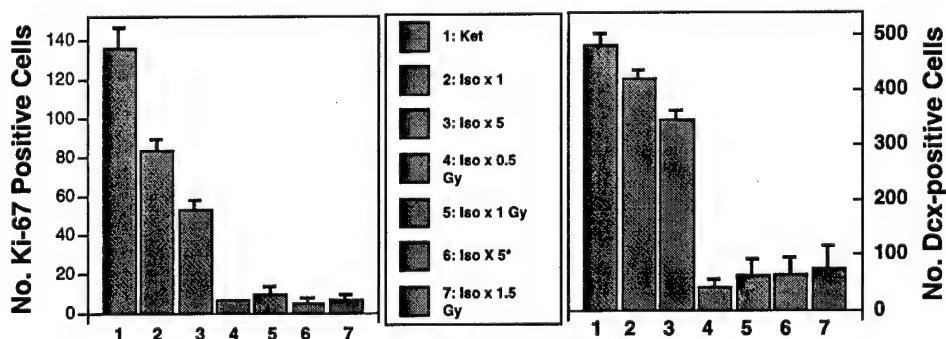

Fig. 13: Effects of fractionated irradiation on proliferating cells (left) and their progeny, immature neurons (right). Isoflurane anesthesia was used for all treatments, which consisted of 5 equal fractions of either 0.5 Gy (lane 4), 1.0 Gy (lane 5) or 1.5 Gy (lane 7). A single isoflurane anesthesia with no irradiation (lane 2) or 5 daily isoflurane treatments with no irradiation (lane 3) significantly reduced cell numbers relative to injectable ketamine + medetomidine (lane 1). A single dose of 5 Gy was given on the last of 5 days of isoflurane anesthesia (lane 6) to compare with the same total dose given in 5 equal fractions (lane 5); no significant dose sparing was observed. There was no apparent difference in cell depletion between the total fractionated doses of 2.5 Gy, 5 Gy or 7.5 Gy.

shown in **Fig. 13**. Surprisingly, these data show that relative to a single anesthesia with ketamine/medetomidine, a single isoflurane treatment induced a significant reduction in proliferating cells (~40%) and immature neurons (~ 15%). Multiple isoflurane anesthesias decreased the cell populations even more **(Fig. 13)**. Additionally, there was little if any sparing effect when a total dose of 5 Gy was fractionated. Finally, the effects of the different fractionated total doses were not different with respect to the adverse effects on proliferating cells and immature neurons. This last result was most striking because in most cell/animal systems, fractionation of dose results in a significant sparing effect due to repair of radiation-induced DNA damage. This result, along with

our recently published data regarding apoptosis (2) in the dentate SGZ, highlights the exquisite radiation sensitivity of these cells to low doses of x-rays.

Given the significant toxic effects of isoflurane on the cells of the SGZ we initiated pilot studies using gentle restraint without anesthesia. Mice were placed is a plastic rodent restraint cone, a thin plastic cone-shaped bag, open at one end, and subjected to head only irradiation. The total radiation time was approximately 1-2 minutes depending upon dose, so the mice were restrained for about 1.5-2.5 minutes, total. A single daily dose of either 1 or 2 Gy was given on 5 consecutive days; tissues were collected 48 hr after the last treatment. Controls consisted of a single restraint each day for 5 days but with no irradiation. In addition a group of mice underwent daily restraint and on the last day they received a single dose of 5 Gy to compare with the mice that received fractionated irradiation. Daily restraint resulted in a decrease in number of proliferating cells and immature neurons. While there was some dose sparing with fractionation for proliferating cells under conditions of restraint, there was no sparing in terms of immature neurons. Furthermore, there was no apparent dose response (**Fig. 14**). These results again show the sensitivity of the cells of the SGZ. Furthermore since no anesthetic was used it is apparent that the stress associated with restraint/irradiation has a major impact on these cells. Other investigators have shown that stress is a negative regulator of neurogenesis (17, 18), but to our knowledge no one has shown such a sensitivity as we have seen in our studies.
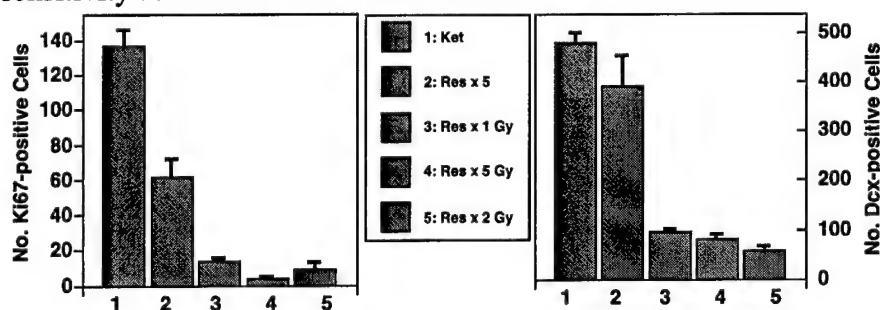

Fig. 14: Effects of restraint and fractionated irradiation on proliferating cells (left) and their progeny, immature neurons (right). Gentle restraint was used for all treatments, which consisted of 5 equal fractions of either 1.0 Gy (lane 3) or 2.0 Gy (lane 5). Five daily restraints with no irradiation (lane 2) significantly reduced cell numbers relative to injectable ketamine + medetomidine (lane 1). A single dose of 5 Gy was given on the last of 5 days of restraint (lane 4) to compare with the same total dose given in 5 equal fractions (lane 3); some dose sparing was observed for proliferating cells. There was no apparent difference in cell depletion between the total fractionated doses of 5 Gy (lane 3) or 10 Gy (lane 5).

Overall, our studies of the radiation response of SGZ cells after fractionated irradiation have provided some interesting and unexpected results regarding the sensitivity of the proliferating precursor cells and their progeny. At least with respect to our relatively acute endponts, there does not seem to be any apparent sparing due to dose fractionation, which suggests that small doses will combine in an additive fashion. Thus, in our experimental design, single doses are equally effective to the more technically demanding and stressful multiple treatment paradigm originally proposed. We do not yet know if the lack of fractionation effect will translate into a similar type of result in longer term assessments of neurogenesis. However, we recently have reported that dose-related changes in neurogenesis observed months after irradiation parallel the dose responses in SGZ cellularity seen as early as 48 hr after irradiation (2). Thus, we expect that radiation-induced changes in neurogenesis and cognitive impairments will be the same after a single dose or the same total dose fractionated over a 1-2 week period. However, this has not yet been shown, so we currently have studies underway assessing neurogenesis after fractionated doses of x-rays.

Key Research Accomplishments:

- Low to medium doses of x-rays significantly decrease the numbers of proliferating neural precursor cells and their progeny, immature neurons, in the dentate SGZ;
- Elevated levels of oxidative stress and indicators of inflammation are observed in the dentate gyrus after irradiation and may play a critical role in the altered neurogenesis seen weeks-months after exposure;

- Studies of neural precursor cell in culture confirm the presence of functional radiation-induced cell cycle checkpoints, which is consistent with a DNA damage response;

- *In vitro* and *in vivo* studies have established that p53 plays a role in the radiation response of neural precursor cells;

- Neural precursor cells *in vitro* are predisposed to redox sensitive changes that are responsive to density dependent cues that regulate ROS and antioxidant levels to control cellular proliferation;

- *In vivo*, when normal precursor cell densities are decreased by low doses of irradiation, elevated levels of oxidative stress are observed which are temporally associated with increased cell proliferation;

- Antioxidant treatment of neural precursor cells in culture with an SOD mimetic drug (Euk-134) leads to *increased* ROS. Use of Euk-134 *in vivo* showed no apparent effects in terms of reducing the impact of x-rays on the precursor cell population in the dentate SGZ. These *in vitro* and *in vivo* results may preclude the use of this type of agent for the management or prevention of radiation-induced damage to neural precursor cells;

- Antioxidant treatment of neural precursor cells in culture with α-lipoic acid reverses the density dependent changes observed in culture; this compound may provide an effective means of reducing the impact of ROS after radiation damage;

- Inhalent anesthetics or gentle restraint (stress) during fractionated irradiation induces loss of proliferating neural precursor cells and immature neurons;

- Little if any sparing of neural precursor cells was obtained by fractionating radiation dose;

- Results from the fractionation studies suggest that the effects of multiple small doses are additive and that for a given dose, single or multiple exposures are equally effective in depleting proliferating precursor cells and their progeny.

REPORTABLE OUTCOMES:

Papers*

1. Monje ML, Mizumatsu S, Fike JR, Palmer TD. Irradiation induced neural precursor-cell dysfunction. **Nat. Med**. 8: 955-962, 2002.

2. Mizumatsu S, Monje ML, Morhardt D, Rola R, Palmer TD, Fike JR. Extreme sensitivity of adult neurogenesis to low doses of X-irradiation. **Can. Research**. 63: 4021-4027, 2003.

3. Limoli CL, Giedzinski E, Rola R, Otsuka S, Palmer TD, Fike JR. Radiation response of neural precursor cells: linking cellular sensitivity to cell cycle checkpointsm, apoptosis and oxidative stress. **Radiation Research,** Submitted.

4. Raber J, Rola R, LeFevour A, Morhardt D, Curley J, Mizumatsu S, Fike JR. Radiation-induced cognitive impairments are associated with changes in hippocampal neurogenesis. **J. Neuroscience,** Submitted.

Only published papers are submitted as appendices.

Abstracts:

1. Mizumatsu S, Morhardt D, Rola R. Monje ML, Palmer TD, Fike JR. Neural precursor cells are extremely sensitive to ionizing irradiation. Neuro-Oncology 4: 356, 2002.

2. Fike JR, Mizumatsu S, Morhardt D, Rola R, Raber J. Ionizing radiation caused long-term inhibition of neurogenesis in the dentate gyrus. J. Neurochem. 85 (Suppl 1), 3, 2003.

CONCLUSIONS:

The studies reported this year give further quantitative support that proliferating precursor cells and their progeny are extremely sensitive to irradiation. Coupled with our neurogenesis data this sensitivity may play a critical role in late developing cognitive impairment after exposure to modest doses of ionizing radiation. Our extensive *in vitro* studies suggest that ROS play a major role in the sensitivity of neural precursor cells, and may act in concert with p53 and cell cycle dependent processes. Our finding that conditions of reduced cell density, such as that seen after radiation-induced cell depletion, are associated with increased ROS is a novel and potentially critical finding with respect to how surviving cells respond to cell loss. The resultant stimulation of ROS-dependent proliferation may be an essential component with respect to the ultimate recovery of neural and other primary progenitor cells after protracted radiation exposure. Unregulated proliferation may result in the fixation of radiation-induced damage, and impair long-term functionality that may have deleterious consequences to cognitive function. Modulating ROS using antioxidant compounds may provide the means to control proliferation in damaged cells, thereby allowing for repair and recovery after radiation injury. Our *in vitro* studies show that antioxidant treatment can, in fact, reverse some of the density-related effects, and ongoing studies both in culture and in animals are testing the ability of such treatment to modulate the extent of injury in neural precursor cells.

As part of our original experimental design we proposed to use multiple small doses delivered over a 1-2 week period to simulate a battlefield exposure. Studies were done this year to address this, and in the course of the experiments, we found that there was little if any biological sparing when a given dose was fractionated. This suggests that the effectiveness of multiple doses is additive, and that from an experimental perspective a single dose will be just as informative and relevant as a fractionated paradigm. Furthermore, we showed that technical considerations such as anesthesia and stress have a profound effect on the survival of neural precursor cells and their progeny. This again highlights the exquisite sensitivity of these cells to toxic agents and provides additional rationale for studying their response and how the loss of these cells can negatively impact individuals exposed to stressful situations (such as battlefield scenarios) combined with cytotoxic agents such as ionizing irradiation.

Given the extreme sensitivity of neural precursor cells we have begun to address specific mechanistic factors that are not only associated with oxidative processes, but that may provide additional targets for interventional treatment. Cell cycle perturbations, p53, mitochondrial influences and the role of inflammation, among others, all appear to play a role in the response of neural precursor cells to irradiation, and may provide insight into the methods/approaches that might minimize the adverse impact of low dose radiation exposure. In the coming year we will address how some of these factors, along with anti-oxidant treatment, affect neurogenesis and ultimately cognitive function. The ability to ameliorate non-lethal radiation effects would not only provide a potential protective strategy for military personnel exposed to moderate doses of irradiation, but also could have a clinical impact on patients undergoing therapeutic irradiation involving the brain.

REFERENCES:

1.   Palmer, T. D., Takahashi, J., and Gage, F. H. The adult rat hippocampus contains primordial neural stem cells. Mol Cell Neurosci, *8:* 389-404, 1997.

2.   Mizumatsu, S., Monje, M. L., Morhardt, D. R., Rola, R., Palmer, T. D., and Fike, J. R. Extreme sensitivity of adult neurogenesis to low doses of x-irradiation. Can Res, 2003.

3.   Tada, E., Parent, J. M., Lowenstein, D. H., and Fike, J. R. X-irradiation causes a prolonged reduction in cell proliferation in the dentate gyrus of adult rats. Neuroscience, *99:* 33-41, 2000.

4.   Murnane, J. P. Cell cycle regulation in response to DNA damage in mammalian cells: a historical perspective. Cancer Metastasis Rev, *14:* 17-29, 1995.

5.   Lotem, J., Peled-Kamar, M., Groner, Y., and Sachs, L. Cellular oxidative stress and the control of apoptosis by wild-type p53, cytotoxic compounds, and cytokines. Proc Natl Acad Sci U S A, *93:* 9166-9171, 1996.

6.   Iyer, R. and Lehnert, B. E. Low dose, low-LET ionizing radiation-induced radioadaptation and associated early responses in unirradiated cells. Mutat Res, *503:* 1-9, 2002.

7.   Berridge, M. V. and Tan, A. S. High-capacity redox control at the plasma membrane of mammalian cells: trans-membrane, cell surface, and serum NADH-oxidases. Antioxid Redox Signal, *2:* 231-242, 2000.

8.   Levin, E. D., Brady, T. C., Hochrein, E. C., Oury, T. D., Jonsson, L. M., Marklund, S. L., and Crapo, J. D. Molecular manipulations of extracellular superoxide dismutase: functional importance for learning. Behav Genet, *28:* 381-390, 1998.

9.   Doctrow, S. R., Huffman, K., Marcus, C. B., Tocco, G., Malfroy, E., Adinolfi, C. A., Kruk, H., Baker, K., Lazarowych, N., Mascarenhas, J., and Malfroy, B. Salen-manganese complexes as catalytic scavengers of hydrogen peroxide and cytoprotective agents: structure-activity relationship studies. J Med Chem, *45:* 4549-4558, 2002.

10.   Kee, N., Sivalingam, S., Boonstra, R., and Wojtowicz, J. M. The utility of Ki-67 and BrdU as proliferative markers of adult neurogenesis. J Neurosci Methods, *115:* 97-105, 2002.

11.   Nacher, J., Crespo, C., and McEwen, B. S. Doublecortin expression in the adult rat telencephalon. Eur J Neurosci, *14:* 629-644, 2001.

12.   Monje, M. L., Mizumatsu, S., Fike, J. R., and Palmer, T. D. Irradiation induces neural precursor-cell dysfunction. Nat Med, *8:* 955-962, 2002.

13.   Chang, S. C., Kao, M. C., Fu, M. T., and Lin, C. T. Modulation of NO and cytokines in microglial cells by Cu/Zn-superoxide dismutase. Free Radic Biol Med, *31:* 1084-1089, 2001.

14.   Chiang, C. S., McBride, W. H., and Withers, H. R. Radiation-induced astrocytic and microglial responses in mouse brain. Radiother. Oncol., *29:* 60-68, 1993.

15.   Daigle, J. L., Hong, J. H., Chiang, C. S., and McBride, W. H. The role of tumor necrosis factor signaling pathways in the response of murine brain to irradiation. Cancer Res, *61:* 8859-8865, 2001.

16.   Vallieres, L., Campbell, I. L., Gage, F. H., and Sawchenko, P. E. Reduced hippocampal neurogenesis in adult transgenic mice with chronic astrocytic production of interleukin-6. J Neurosci, *22:* 486-492, 2002.

17.   Gould, E. and Tanapat, P. Stress and hippocampal neurogenesis. Biol Psychiatry, *46:* 1472-1479, 1999.

18.   Fuchs, E. and Gould, E. Mini-review: in vivo neurogenesis in the adult brain: regulation and functional implications. Eur J Neurosci, *12:* 2211-2214, 2000.

Irradiation induces neural precursor-cell dysfunction

MICHELLE L. MONJE[1], SHINICHIRO MIZUMATSU[2], JOHN R. FIKE[2] & THEO D. PALMER[1]

[1]Department of Neurosurgery, Stanford University, Stanford, California, USA
[2]Department of Neurological Surgery, University of California San Francisco, San Francisco, California, USA
Correspondence should be addressed to T.D.P.; email: tpalmer@stanford.edu

In both pediatric and adult patients, cranial radiation therapy causes a debilitating cognitive decline that is poorly understood and currently untreatable. This decline is characterized by hippocampal dysfunction, and seems to involve a radiation-induced decrease in postnatal hippocampal neurogenesis. Here we show that the deficit in neurogenesis reflects alterations in the microenvironment that regulates progenitor-cell fate, as well as a defect in the proliferative capacity of the neural progenitor-cell population. Not only is hippocampal neurogenesis ablated, but the remaining neural precursors adopt glial fates and transplants of non-irradiated neural precursor cells fail to differentiate into neurons in the irradiated hippocampus. The inhibition of neurogenesis is accompanied by marked alterations in the neurogenic microenvironment, including disruption of the microvascular angiogenesis associated with adult neurogenesis and a marked increase in the number and activation status of microglia within the neurogenic zone. These findings provide clear targets for future therapeutic interventions.

Radiation therapy is an important adjuvant treatment for primary brain tumors, tumors metastatic to the brain, central nervous system involvement of leukemia/lymphoma and head and neck cancers. Unfortunately, in both pediatric and adult patients, cranial irradiation causes a debilitating cognitive decline. Months to years after treatment, patients that survive their initial disease present with progressively severe deficits in the hippocampal-dependent functions of learning, memory and spatial information processing[1-6]. For most pediatric patients, this cognitive deterioration leads to special education or institutionalization[1]. With increasingly successful cancer treatments in the adult population, there is an alarming rate of dementia in long-term survivors[4,6]. These deficits frequently occur in the absence of overt vasculopathy or demyelination, indicating that a more subtle pathology may be at work.

Radiation-induced learning and memory deficits in animal models[7,8] are accompanied by an increase in hippocampal apoptosis[9,10], a decrease in hippocampal proliferation and a decrease in adult neurogenesis[9,11,12]. It is likely that postnatal neurogenesis plays a critical role in normal hippocampal function[13-15] and that radiation-induced alterations in neurogenesis contribute to cognitive deficits. Differentiation of neural precursor cells depends on a specific neurogenic microenvironment and is influenced by intercellular cues[16-18]. This work explores whether inhibition of hippocampal neurogenesis following irradiation is simply a function of neural progenitor-cell depletion, or reflects more profound changes in the neurogenic microenvironment.

Model of cranial radiation therapy

A rat model of 10-Gray (Gy), single-dose, whole-brain cranial radiation exposure with body shielding was used to explore the effects of radiation on adult neurogenesis. A single 10-Gy x-ray irradiation dose to rat brain is well below the threshold for frank vascular changes, demyelination or radionecrosis[7,19]. Because rat brain is more resistant to radiation injury than human brain, a 10-Gy dose in the rat approximates a clinically relevant dose in humans[19-22]. Effects on hippocampal progenitor cell biology were examined one or two months after radiation exposure.

In many of our experiments, we used the thymidine analogue bromodeoxyuridine (BrdU) to label proliferative cells. BrdU is incorporated into DNA during both DNA synthesis and repair. A theoretical complication thus exists as increased rates of DNA repair would be expected in irradiated tissue. A previous study using ionizing radiation to induce DNA damage demonstrated that the methods used in this work are not sensitive enough to detect BrdU incorporated during DNA repair[23].

Irradiation inhibits neural precursor cell proliferation

Hippocampal cell proliferation is reduced following cranial irradiation[9]. To confirm this result, animals were given six daily BrdU injections to label proliferating cells at one month after irradiation and killed 3–4 weeks later (that is, at two months post-radiation exposure). The number of surviving BrdU-labeled cells was quantified in the dentate gyrus and underlying subgranule zone of the hippocampus (Fig. 1a–c) using immunohistochemical staining of BrdU and unbiased stereological counting methods[24]. We scored the granule cell layer, including the subgranule zone, and the hilus of the dentate gyrus. The number of newborn cells in the irradiated granule-cell layer and hilus was decreased to 38% ($P < 0.005$) and 52% ($P < 0.02$), respectively, relative to non-irradiated levels ($n = 4$) (Fig. 1d).

The reduction in cell proliferation/survival could be due to radiation-induced acute ablation of the precursor population, impaired growth potential or impaired mitogenic signaling of
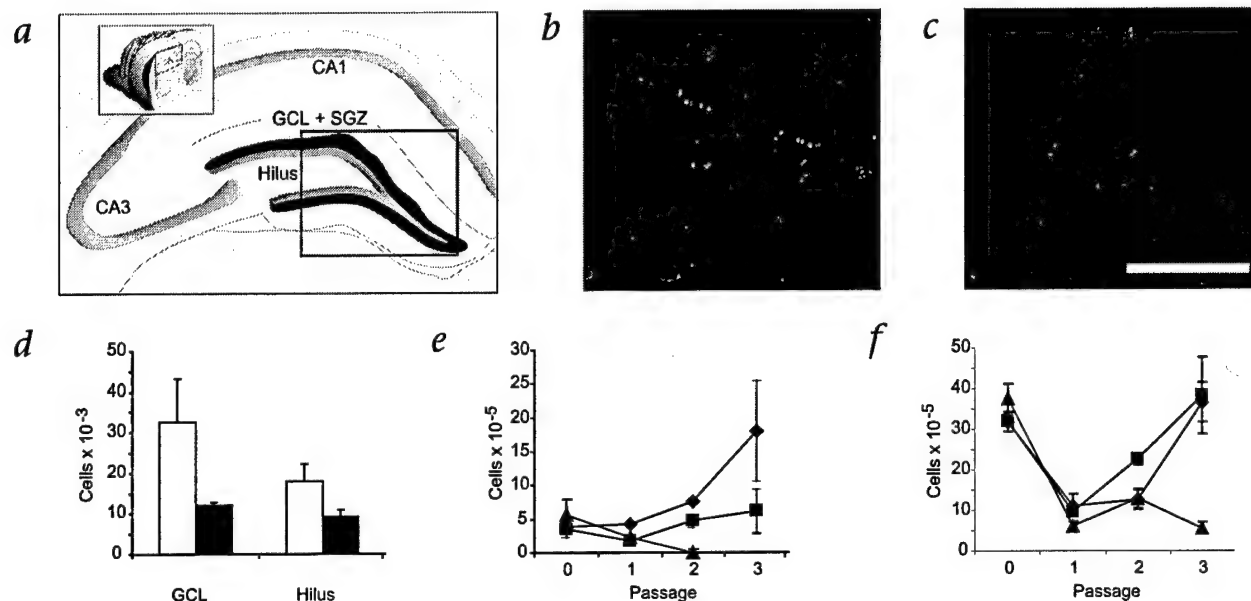
018

Fig. 1 Irradiation decreases neural precursor proliferation and growth potential. **a,** Inset shows the caudal half of a rat brain coronally bisected to expose the dorsal-medial poles of the hippocampal formations (red box outlines the right hippocampal formation shown in panel). The hippocampal formations are banana-shaped structures that extend caudally and ventrally from this plane. The regions within the hippocampus scored for this study include the hilus, the granule cell layer (GCL, blue) and the subgranule zone (SGZ, green), which is a thin lamina at the boundary of the GCL and hilus. Cell counts were made within the indicated GCL including a 50-μm hilar margin of the SGZ (blue and green areas combined) or within the hilus, **b** and **c,** Confocal micrograph (×10 magnification, zoom of 1) of the dentate gyrus in a control animal (**b**) and an irradiated animal (**c**). NeuN (mature neurons) are shown in blue; BrdU (proliferative cells) are green. Scale bar, 200 μm. **d,** Radiation-induced suppression of proliferation is documented by scoring the total number of BrdU⁺ cells per GCL/SGZ and hilus of the entire hippocampal dentate gyrus in control animals (□) and at two months post-irradiation (■). Data are means ± s.e.m.; n = 4 animals per group. **e - f,** Precursor cell growth in culture. Adult rats were sacrificed one month after exposure to 0 Gy (◆), 2 Gy (■) or 10 Gy (▲) and hippocampi (**e**) or whole brain (**f**) were used to establish cultures highly enriched for precursor cells (n = 3 animals per group).

the hippocampal environment. To determine viability and growth potential following irradiation, we cultured precursor cells from the hippocampus and whole-brain one month after exposure to 0, 2 or 10 Gy irradiation. Irradiated and non-irradiated brains yielded an equivalent number of viable precursors (3.9 × 10⁵ cells per hippocampal pair in normal animals versus 5.6 × 10⁵ cells in 10-Gy irradiated animals; P = 0.52; n = 3 independent cultures from separate animals). This result indicates that an acute ablation of precursor cells does not occur. However, precursor growth *in vitro* was impaired in a dose-dependent manner (Fig. 1e and f). The virtual depletion of neural progenitor cells exposed to 10 Gy irradiation likely reflects radiation-induced mitotic catastrophes occurring over the course of multiple cell divisions.

Irradiation alters the cell fate profile *in vivo*

To examine the *in vivo* cell fate profile of the remaining proliferative population, animals were given six daily BrdU injections at one month post-irradiation and killed 3–4 weeks later, a time when most of the BrdU-labeled precursors in the normal hippocampus would have differentiated into granule-cell neurons[25]. Proliferative cell fate was determined using immunofluorescent staining and confocal microscopy. The percent of BrdU-labeled cells that adopt a particular cell fate is shown in Fig. 2a. The total number of newborn cells of each phenotype was also estimated by correcting the proportion of each BrdU-labeled cell type for total number of BrdU⁺ cells per hippocampal dentate gyrus (Fig. 2b).

We found a 97% reduction in newborn neurons two months after cranial irradiation (P < 0.004; n = 4) (Fig. 2a–d), whereas the production of astrocytes and oligodendrocytes was relatively spared. There was no significant difference in the proportions of newborn astrocytes (P = 0.56; n = 4) (Fig. 2a and e) or endothelial cells (P = 0.08; n = 4) (Fig. 2a and g). There was a relative increase in the percent of cells adopting an immature oligodendrocyte phenotype after irradiation (177% of control; P < 0.003; n = 4) (Fig. 2a and f). However, this did not correspond to an increase in the total number of oligodendrocytes (Fig. 2b). There was a decrease in the absolute number of all newborn cell types following cranial irradiation. The one notable exception was a striking increase in the number of proliferative microglia. Activated microglia, the resident immune cells of the brain, accounted for 22 ± 6.8% of the BrdU-labeled cells in the irradiated hippocampus, but were virtually absent from the proliferative population of control brains (P < 0.009; n = 4) (Fig. 2a and h).

Irradiated precursors differentiate into neurons *in vitro*

To investigate whether radiation-induced failure of *in vivo* neurogenesis could be due to a defect intrinsic to progenitor cells, we investigated the potential of irradiated progenitor cells to differentiate into neurons when removed from the environment of the irradiated brain. Primary cultures isolated from brains one month after 0, 2 or 10 Gy radiation exposure (Fig. 1) were allowed to differentiate for 5 days following growth factor removal and stimulation with retinoic acid. Immunofluorescent staining
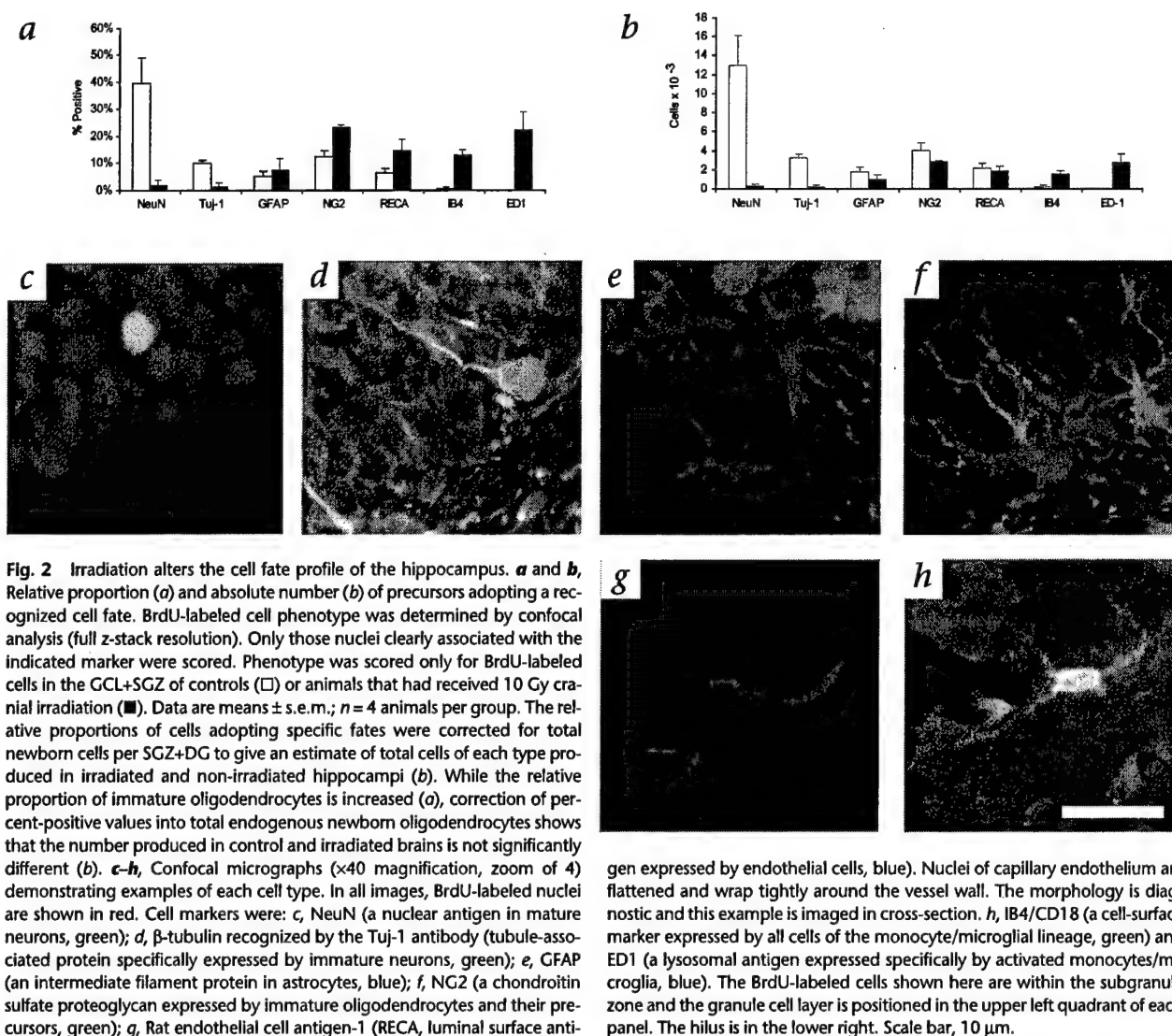
Fig. 2 Irradiation alters the cell fate profile of the hippocampus. *a* and *b*, Relative proportion (*a*) and absolute number (*b*) of precursors adopting a recognized cell fate. BrdU-labeled cell phenotype was determined by confocal analysis (full z-stack resolution). Only those nuclei clearly associated with the indicated marker were scored. Phenotype was scored only for BrdU-labeled cells in the GCL+SGZ of controls (□) or animals that had received 10 Gy cranial irradiation (■). Data are means ± s.e.m.; *n* = 4 animals per group. The relative proportions of cells adopting specific fates were corrected for total newborn cells per SGZ+DG to give an estimate of total cells of each type produced in irradiated and non-irradiated hippocampi (*b*). While the relative proportion of immature oligodendrocytes is increased (*a*), correction of percent-positive values into total endogenous newborn oligodendrocytes shows that the number produced in control and irradiated brains is not significantly different (*b*). *c–h*, Confocal micrographs (×40 magnification, zoom of 4) demonstrating examples of each cell type. In all images, BrdU-labeled nuclei are shown in red. Cell markers were: *c*, NeuN (a nuclear antigen in mature neurons, green); *d*, β-tubulin recognized by the Tuj-1 antibody (tubule-associated protein specifically expressed by immature neurons, green); *e*, GFAP (an intermediate filament protein in astrocytes, blue); *f*, NG2 (a chondroitin sulfate proteoglycan expressed by immature oligodendrocytes and their precursors, green); *g*, Rat endothelial cell antigen-1 (RECA, luminal surface anti-

gen expressed by endothelial cells, blue). Nuclei of capillary endothelium are flattened and wrap tightly around the vessel wall. The morphology is diagnostic and this example is imaged in cross-section. *h*, IB4/CD18 (a cell-surface marker expressed by all cells of the monocyte/microglial lineage, green) and ED1 (a lysosomal antigen expressed specifically by activated monocytes/microglia, blue). The BrdU-labeled cells shown here are within the subgranule zone and the granule cell layer is positioned in the upper left quadrant of each panel. The hilus is in the lower right. Scale bar, 10 μm.

demonstrated that precursors from both normal and irradiated brains were able to differentiate into immature neurons and glia (Fig. 3*a–d*). Contrary to expectations, the 10 Gy cultures contained a higher number of differentiated cells than control or 2 Gy cultures. Although the total number of differentiated cells increased, the ratio of neurons to glia was not different (neurons / astrocytes + oligodendrocytes = 1.7 versus 1.5, respectively). Furthermore, immature type-III β tubulin–expressing neurons from 10-Gy irradiated brains were morphologically distinct with larger soma and more long thin processes (Fig. 3*d*). The significance of this morphological difference is not yet known but it is possible that cell-cycle arrest induced by radiation damage may promote neural precursor differentiation.

Non-irradiated grafts do not differentiate *In vivo*
The ability of irradiated precursor cells to differentiate into neurons *in vitro* suggests that reduced neurogenesis following radiation exposure may not be merely a function of reduced progenitor-cell number or proliferative activity. Loss of neurogenesis may also reflect an alteration in neural stem-cell fate.

To explore the hypothesis that alterations in the neurogenic microenvironment contribute to the inhibition of neurogenesis, we stereotaxically transplanted highly enriched non-irradiated neural stem/precursor cells into the dentate gyrus one month after irradiation. As above, we killed the animals 3–4 weeks later and examined grafted cell fate at two months after irradiation. The grafted cells were labeled with BrdU before transplant[26,27] and the fate of the transplanted cells was analyzed with immunohistochemistry and confocal microscopy (Fig. 4). Although transplanted cell survival is comparable in control and irradiated animals (Fig. 4*a* and *b*), differentiation of grafted stem/precursor cells into neurons (Fig. 4*d* and *e*) was reduced by 81% in the irradiated brain relative to control, indicating a marked disruption of the microenvironment necessary to support neurogenesis (24.7% NeuN- + Tuj1-positive in controls versus 4.6% NeuN + Tuj1 positive in 10 Gy-irradiated animals; $P < 0.005$; $n = 3$). In contrast, gliogenesis in the grafted stem/precursor cells was preserved in the irradiated hippocampus, with an equal proportion of stem/precursor cells adopting an astrocyte fate (Fig. 4*f*) and a moderate increase in the rela-
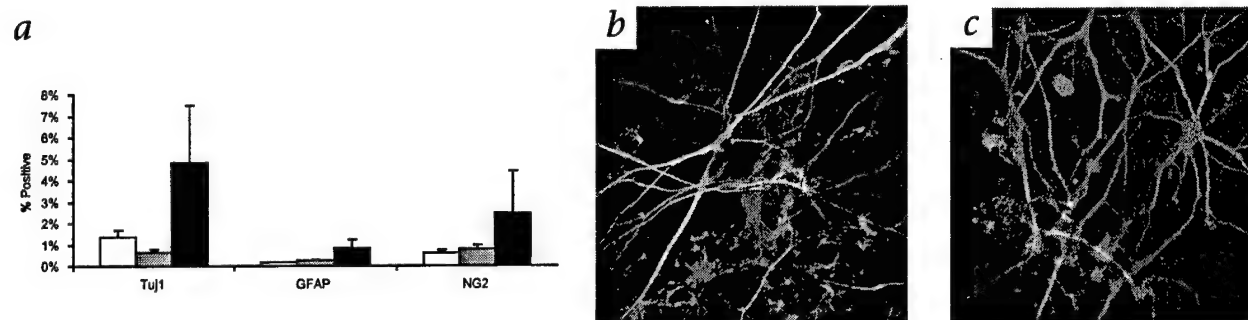
Fig. 3 Precursor cells from irradiated brains can differentiate into neurons *in vitro*. **a**, Differentiation of precursor cells isolated from animals exposed to 0 Gy (□), 2 Gy (▨) or 10 Gy (■) cranial radiation. Data are means ± s.e.m.; *n* = 3 animals per group. **b–d**, Confocal micrographs of precursor cells isolated from brains exposed to either 0 Gy (*b*), 2 Gy (*c*) or 10 Gy (*d*) that were cultured for 5 d under differentiation conditions. Cells were immunostained for type III β-tubulin (immature neurons, green), GFAP (astrocytes, red) and NG2 (immature oligodendrocytes, blue). Scale bar, 50 µm.

tive proportion of stem/precursor cells expressing an immature oligodendrocyte phenotype (NG2; Fig. 4*g*) relative to control (*P* < 0.05, *n* = 3).

Irradiation increases activated microglia

Expression of pro-inflammatory cytokines has been shown to increase acutely in response to cranial irradiation[28]. Mounting evidence suggests that microglial activation, and resultant cytokine expression, influences neural precursor cell prolifera-

tion and fate[18], and hippocampal function[29]. To determine if a chronic inflammatory response is correlated with inhibition of neurogenesis, we examined microglial activation at two months after irradiation. In addition to the increase in proliferative microglia (Fig. 2*a*, *b* and *h*), there was also an overall increase in the absolute number of activated microglia (Fig. 5*a–d*). Radiation induced a 250% in-
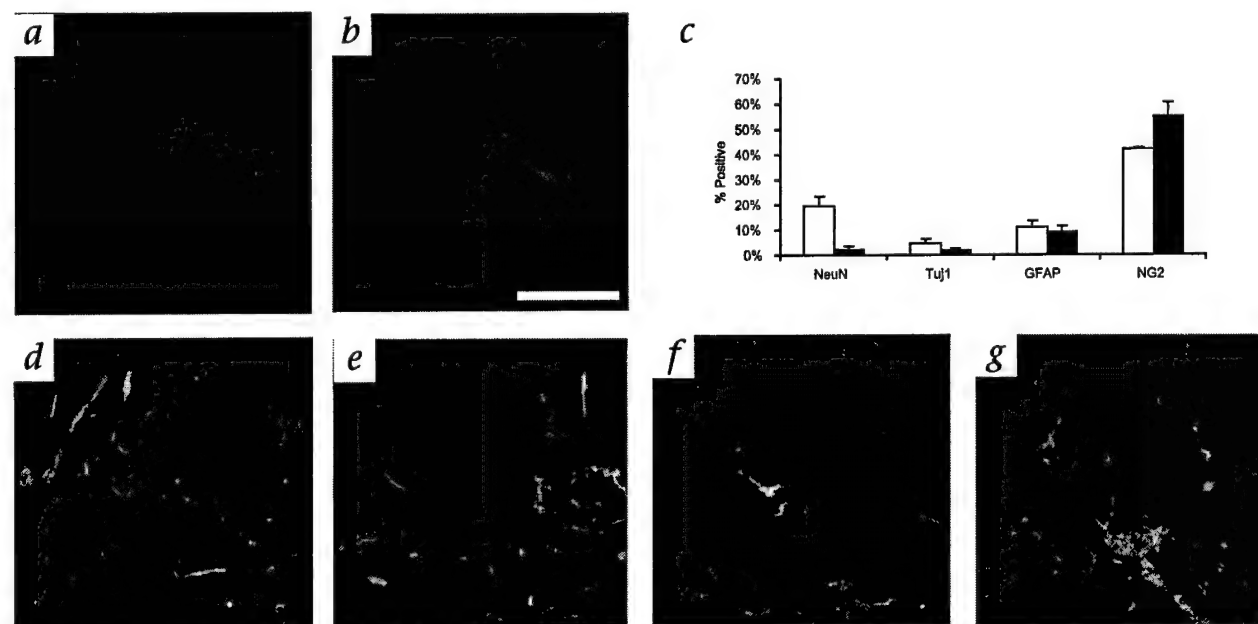

Fig. 4 Irradiation disrupts the neurogenic microenvironment. *a* and *b*, Non-irradiated neural stem/precursor cells were transplanted into the dentate gyrus of non-irradiated (*a*) and irradiated (*b*) animals. Transplanted cells were pre-labeled with BrdU. Low-power confocal micrographs show an overview of the surviving cells within the hippocampus. *a*, Non-irradiated hippocampus stained for NeuN (mature neurons, blue) and BrdU (transplanted cells, red). *b*, 10 Gy-irradiated hippocampus stained for NG2 (immature oligodendrocytes, blue) and BrdU (transplanted cells, red). Distributions of transplanted cells are roughly equivalent in control and irradiated hippocampi. *c*, Cell-fate profile of neural stem/precursors transplanted to the normal (□) or 10 Gy (■) irradiated hippocampus (*n* = 3 animals per group). *d–g*, Confocal micrographs of transplanted cells. *d*, mature neuron (NeuN, blue; BrdU, red); *e*, immature neuron (Tuj-1, green; BrdU, red); *f*, astrocyte (GFAP, blue; BrdU, red); *g*, immature oligodendrocyte (NG2, green; BrdU, red). Scale bars, 200 µm (*a* and *b*) and 10 µm (*d–g*). The tissues surrounding the transplanted cells shown in *d–g* were also reconstructed in three dimensions (see Supplementary information).

crease in total activated microglia per hippocampus in both the granule cell layer ($P < 0.005$) and the hilus ($P < 0.02$; $n = 4$). This increase may reflect increased microglial proliferation, recruitment and/or survival, and speaks to a dramatic chronic inflammatory response following cranial radiation exposure.

Irradiation alters the neuro-angiogenic relationship

Previous work has highlighted the importance of the anatomical and signaling relationships between neural precursor cells and the microvasculature of neurogenic regions[17,23,30]. Proliferative precursor cells in the adult hippocampus tend to be clustered around small vessels. Recruitment of the precursor cells is accompanied by a synchronous stimulation of microvascular angiogenesis and this relationship is thought to be important to normal neurogenesis[23]. The focal accumulation of precursors as clusters within the vascular niche is evident after one week of BrdU labeling, but the labeled cells rapidly migrate away from these foci and are not observed as clusters at later time points. We therefore examined the hippocampal microanatomy in rats killed immediately after six daily BrdU injections given one month after irradiation. The BrdU-labeled cells in control animals clustered on and around the microvasculature as reported[23] (Fig. 6a and c). This association was lost in the irradiated hippocampus (Fig. 6b and d). Measurements of the distance between BrdU-labeled cells and the nearest vessel support this observation (Fig. 6e). We examined a 1-in-12 series through the hippocampus of representative animals, and found that the average distance from the midpoint of a BrdU-labeled nucleus to the nearest vessel was increased from 5.7 ± 0.6 μm in controls to 11.9 ± 1.3 μm in irradiated animals ($P < 0.0001$). Activated microglia comprise a significant proportion of the proliferative population of the irradiated hippocampus, but are absent from the controls. To avoid the confounding presence of proliferative microglia, reactive monocyte/microglial cells (ED-1⁺) were identified by immunofluorescent staining and were excluded from the distance measurements in Fig. 6e. The inclusion of microglia in the measurement would not have changed the result given that microglia (when measured independently) also showed a near-random distribution within the subgranule zone and granule-cell layer relative to the vasculature (11.3 ± 1.9 μm to the nearest vessel).

In addition, irradiation disrupted the normal clustering of cells in proliferative foci around the vasculature. The number of cells present in loose clusters within the subgranule zone is plotted against the distance from the middle of the cluster to an adjacent vessel (Fig. 6f). A cluster of 3 cells in a typical perivascular arrangement is illustrated in a control animal (Fig. 6c). Labeled cells in the irradiated hippocampus were only found as individual cells or doublets (Fig. 6d). The disruption of clustering is also clearly evident by eye when comparing the distribution of BrdU-labeled cells along the thin lamina of the subgranule zone (Fig. 6a and b).

Discussion

We have demonstrated that cranial irradiation markedly alters hippocampal progenitor-cell biology. Within the irradiated hip-
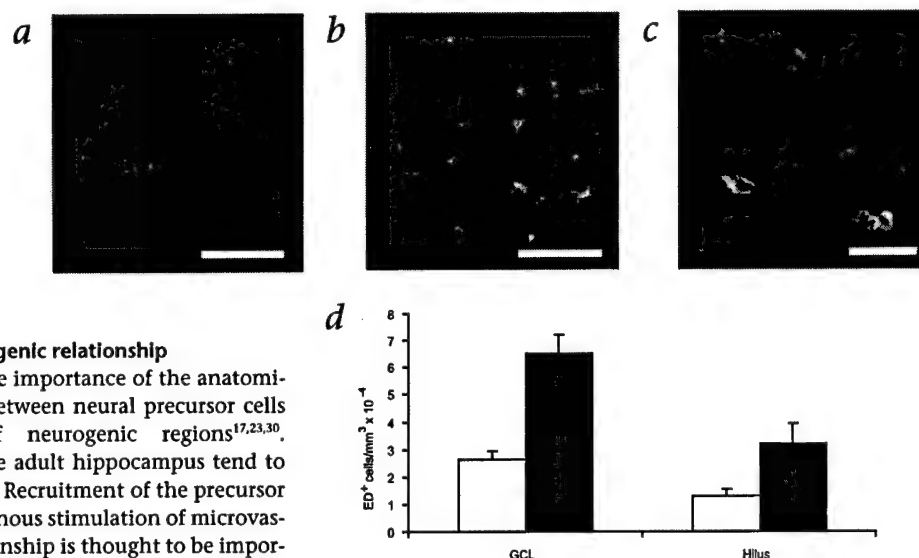

Fig. 5 Irradiation induces a chronic inflammatory response. *a–b* Confocal micrographs demonstrate the increase in activated microglia in the dentate gyrus at two months post-irradiation (*b*) compared with control (*a*). ED1 (activated microglia, green); IB4 (microglia, blue); BrdU (proliferative cells, red). *c,* Detail of activated microglia in the subgranule zone at two months post-irradiation. ED1, red; IB4, blue; BrdU, green. *d,* Quantification of activated microglia (dividing + non-dividing ED1⁺ cells) in the GCL+SGZ in controls (□) and at two months after 10 Gy irradiation (■). Data are means ± s.e.m., $n = 4$ animals per group. Scale bars, 50 μm (*a* and *b*) and 10 μm (*c*).

pocampus, precursor proliferation is reduced by 62% and neurogenesis is almost entirely ablated. The absence of neurogenesis could be due to the dysfunction and/or loss of neuron-restricted precursors or stem cells. Our results suggest that irradiation affects the stem/precursor-cell pool and alters the signaling in the local environment that is necessary for neurogenesis.

Therapeutic radiation is used to eradicate dividing cancer cells and it is conceivable that the neural precursor pool would be similarly ablated in the irradiated brain. Although proliferative activity is reduced, normal numbers of neural progenitor cells can be isolated two months after radiation exposure. This argues against acute precursor-cell ablation as the major cause of the neurogenic defect observed at this time point, but does not preclude a longer-term depletion of neural precursor cells. The neural stem/precursor cells isolated from irradiated hippocampi grew for a short time in culture but failed to expand beyond 2–3 passages. Over time, this mitotic deficiency may lead to a shortage of neural stem/precursor-cells *in vivo*.

Irradiation spares 38% of the proliferative activity within the subgranule zone, yet these cells do not generate neurons. This could be due to the specific ablation of cells that can differentiate into neurons or to a cell-intrinsic defect in irradiated precursors that renders them unable to differentiate into neurons. Our *in vitro* data show that irradiated precursors can differentiate into neurons, and that irradiated precursors generate the same ratio of neurons to glia as control precursors (Fig. 3). This suggests that the defect is due neither to a lack of precursor cells nor to an intrinsic inability to differentiate. However, differentiation was not entirely normal. In the 5-day differentiation paradigm used in the present study, roughly 2% of non-irradiated precursors differentiated sufficiently to express markers for neurons or glia.
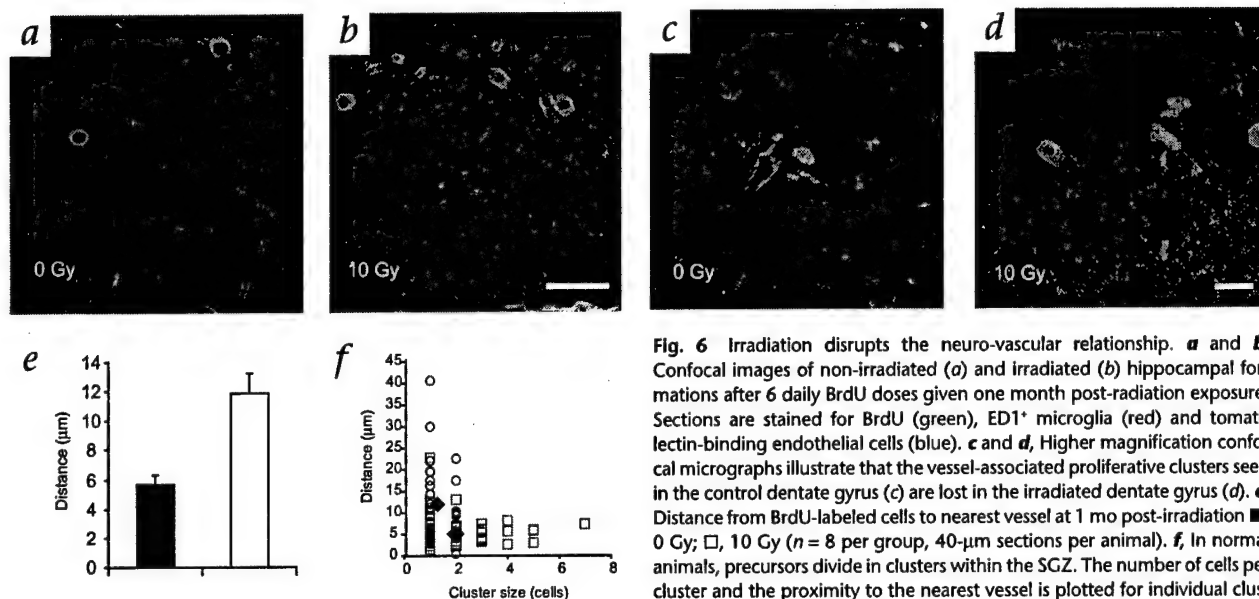
Fig. 6 Irradiation disrupts the neuro-vascular relationship. **a** and **b**, Confocal images of non-irradiated (**a**) and irradiated (**b**) hippocampal formations after 6 daily BrdU doses given one month post-radiation exposure. Sections are stained for BrdU (green), ED1+ microglia (red) and tomato lectin-binding endothelial cells (blue). **c** and **d**, Higher magnification confocal micrographs illustrate that the vessel-associated proliferative clusters seen in the control dentate gyrus (**c**) are lost in the irradiated dentate gyrus (**d**). **e**, Distance from BrdU-labeled cells to nearest vessel at 1 mo post-irradiation ■, 0 Gy; □, 10 Gy (n = 8 per group, 40-μm sections per animal). **f**, In normal animals, precursors divide in clusters within the SGZ. The number of cells per cluster and the proximity to the nearest vessel is plotted for individual clusters in controls (□) and irradiated animals (O). The mean values are also plotted for controls (◆) and irradiated (◆) animals. Error bars for s.e.m. are smaller than the symbol itself. The distance value for each cluster is the average of distances for all cells within a cluster. Scale bars, 200 μm (**a** and **b**) and 10 μm (**c** and **d**).

In contrast, 8% of the cells from irradiated brains differentiated over the same time period and these cells displayed robust neurite elaboration (Fig. 3). This suggests that the basic differentiation machinery may be intact but aberrantly regulated following irradiation.

Although irradiated neural precursors can differentiate into neurons *in vitro*, it is possible that they may be unable to respond to the more refined neurogenic signaling present *in vivo*. Alternatively, irradiated neural precursor cells, though somewhat abnormal, may be fully responsive to normal signaling and the neurogenic signals may simply be absent or overridden in the local microenvironment of the irradiated hippocampus. Since non-irradiated stem/precursor cells transplanted to the irradiated hippocampus generate very few neurons relative to controls (Fig. 4), we surmise that the local signaling within the dentate gyrus is defective and that the decrease in neurogenesis previously observed[9] represents a chronic dysfunction of the neurogenic microenvironment.

Both stem cells and committed neuronal precursors are active within the adult hippocampus, and the alterations in signaling induced by irradiation may affect one or both of these populations. Neurogenesis itself is highly restricted to discrete locations within the adult brain and the production of neurons from multipotent stem cells or their committed progeny is entirely dependent on signaling within these neurogenic zones. Prior transplants of stem cells into the hippocampus demonstrate the importance of this local signaling. When a stem-cell population is injected into the dentate gyrus (Fig. 4a and b), only those cells that migrate into the subgranule zone differentiate into neurons, even though multipotent stem cells and neuron-committed precursors are distributed along a much larger injection tract. Those stem/precursor cells that remain outside of the subgranule zone generate only glia[26,27]. The relative role of differential survival versus instruction in this context is not known. However, a similar precise anatomical restriction is seen in multipotent stem-cell transplants to the subependymal zone and rostral migratory stream[26,27,31], suggesting that adult neurogenesis requires both competent cells and appropriate local signaling.

Following irradiation, the subgranule zone may no longer instruct multipotent stem cells to adopt a neuronal fate. If this were true, then one could overcome the deficit with transplants of committed neuroblasts. Alternatively, the signals specific for recruiting committed neuroblasts may be missing or blocked. If this were true, then neither transplants of committed cells nor multipotent stem cells would generate new neurons. Ongoing studies may provide a clear answer to these questions.

The mechanisms behind post-irradiation neurogenic failure within the subgranule zone remain unknown but may include effects on stem-cell fate as well as changes in the relative amplification or survival of committed neuronal or glial progenitors. Seaberg and van der Kooy[32] suggest that multipotent stem cells reside within the ventricular margins of the hippocampus and not within the subgranule zone proper. This theory is still controversial but, if true, the primary defect may lie in the microenvironment that normally promotes the survival and amplification of neuron-restricted progenitors which divide within the subgranule zone.

Two perturbations in the subgranule zone microenvironment may contribute to radiation-induced failure of neurogenesis. First, the chronic increase in the inflammatory response following irradiation is likely to inhibit neurogenesis via the elaboration of interleukin-6 (ref. 18) and/or other pro-inflammatory cytokines. Second, the normal association between precursor cells and microvasculature is lost, indicating that the focal recruitment of neural precursors in an angiogenic microenvironment is disrupted. We have noted in earlier work that neurons are generated within small clusters of precursors found in close contact with microcapillaries[23], and recent work by Louissant *et al.* has provided additional insights into the role that endothelium plays in adult neurogenesis[30]. The loss of this unique neurogenic anatomy indicates a fundamental disruption of the cellular and molecular interactions that are central to normal

hippocampal progenitor-cell biology[23]. Given the known effects of radiation on endothelium, it seems likely that activation or change in endothelial status may have a central role. Promising avenues of study include evaluation of microglial blockade and reconstitution of normal vascular biology. Undoubtedly, there are additional radiation-induced microenvironmental perturbations influencing neurogenesis that remain unexplored.

Treatment strategies for radiation-induced deficits in cognition will need to address both precursor-cell loss and damage to mechanisms of neurogenesis. It seems probable that successful therapeutic intervention will involve both protection/replacement of the neural progenitor-cell population, as well as drug-based manipulation of microenvironmental factors. The aggressive management of microglial inflammation during and after irradiation may prove to be a feasible and important clinical intervention.

Methods

Irradiation. Adult female Fisher 344 rats were anesthetized with ketamine and xylazine and exposed to cranial irradiation using a Philips orthovoltage X-ray system (Hamburg, Germany) operated at 150 kVp and 20 mA, as described[9]. Briefly, each rat was irradiated individually in a 5×6-cm treatment field with shielding of body, neck, eyes and snout. Only the cranium was unshielded. For 2 Gy, rats were placed in sternal recumbancy and given a single 2-Gy dose. For 10 Gy, rats were placed in lateral recumbancy and, by alternating sides, given sequential 5-Gy doses. Dosimetry was done using a Keithley electrometer ionization chamber (Cleveland, Ohio) calibrated using lithium fluoride thermal luminescent dosimeters. The corrected dose rate was approximately 175 cGy per min at a source to skin distance of 21 cm. Sham-irradiated controls for all experiments received anesthesia only.

BrdU injections and tissue preparation. Animals were injected intraperitoneally with BrdU once a day for 6 d. Animals were then anesthetized and killed on the 7th or 28th day after the initial BrdU injection by transcardial perfusion with 4% paraformaldehyde. Brains were removed and postfixed overnight and then equilibrated in phosphate buffered 30% sucrose. Free-floating 40-μm sections were collected on a freezing microtome and stored in cryoprotectant as described[23]. All animal studies were performed in accordance with NIH guidelines for the humane use of animals and all procedures were reviewed and approved by the Institutional Animal Care and Use Committee.

Immunohistochemistry and immunofluorescent staining. Free-floating sections were immunostained as described[23] using the following primary antibodies and working concentrations: mouse anti-NeuN (1:4; gift from R. Mullen); guinea pig-anti GFAP (1:800; Harlan, Indianapolis, Indiana); mouse anti-type III β tubulin (Tuj-1, 1:500; Berkeley Antibody Co., Richmond, California); rabbit anti-NG2 (1:200; gift from W. Stallcup); mouse anti-rat endothelial cell antigen-1 (RECA-1, 1:20; Pharmingen, San Diego, California); mouse anti-integrin β2 (IB4, direct FITC conjugated, 1:100; Sigma); mouse anti-ED-1 (1:100; Research Diagnostic, Flanders, New Jersey); biotinylated-*Lycopersicon esculentum* (tomato) lectin (1:200; Vector, Burlingame, California).

Confocal microscopy. All confocal microscopy was performed using a Zeiss 510 confocal microscope (Thornwood, New York). Appropriate gain and black-level settings were determined on control tissues stained with secondary antibodies alone. Upper and lower thresholds were always set using the range indicator function to minimize data loss through saturation.

Cell counting and unbiased stereology. All counts were limited to the hippocampal granule cell layer proper and a 50-μm border along the hilar margin that included the neurogenic subgranule zone. The proportion of BrdU cells displaying a lineage-specific phenotype was determined by scoring the colocalization of cell phenotype markers with BrdU using confocal microscopy. Split panel and z-axis analysis were used for all counting. All counts were performed using multi-channel configuration with a ×40 ob-

jective and electronic zoom of 2. When possible, 100 or more BrdU⁺ cells were scored for each marker per animal. Each cell was manually examined in its full 'z'-dimension and only those cells for which the nucleus was unambiguously associated with the lineage-specific marker were scored as positive. Supplemental z-stacks with orthogonal views were provided for review. The total number of BrdU-labeled cells per hippocampal granule cell layer and subgranule zone was determined using diaminobenzadine-stained tissues. Stained BrdU⁺ nuclei (Fig. 1*a*) were scored under light microscopy using Microbrightfield Stereo Investigator software and the Fractionator method. Overestimation was corrected using the Abercrombie method for nuclei with empirically determined average diameter of 13 μm within a 40-μm section. Distance measurements from BrdU-labeled nuclei to the nearest vessel were performed at ×40 magnification and measurements were taken in the x-y plane from the center of a BrdU-labeled nucleus to the edge of the nearest vessel. Proliferative microglia and endothelial cells were excluded from distance measurements.

Progenitor cell culture. Whole hippocampal lobes were dissected from adult female rats that had received 0-, 2-, or 10-Gy cranial irradiation as described[23]. The hippocampal formations were processed in parallel to the remaining whole-brain tissues. Tissues were enzymatically digested with a mixture of papain, neutral protease and DNAse and then fractionated on a Percoll step gradient. Cells floating on a 65–35% interface were collected and plated into laminin-coated dishes in defined medium containing DMDM:F12 (1:1), N2 supplement (Gibco, Carlsbad, California) and 20 ng per ml FGF-2 (Peprotech, Rocky Hill, New Jersey). Cultures were passaged in parallel when reaching confluence and total viable cell counts were made using a hemocytometer to score Trypan blue-excluding cells at each passage. The transplanted cells were derived from a primary culture and transplanted after roughly 10 population doublings *in vitro*. A clonal analysis previously done on this population indicated that roughly 23% of the cells were multipotent and self-renewing.

Statistics. Unpaired, two-tailed Student's t-tests were used in all comparisons.

Note: Supplementary information is available on the Nature Medicine *website.*

1. Strother, D.R. *et al.* Tumors of the central nervous system. in *Principles and Practice of Pediatric Oncology*, 4th edn. (eds. Pizzo, P.A. & Poplack, D.G.) 751–824 (Lippincott Williams and Wilkins, Philadelphia, Pennsylvania, 2002).
2. Surma-aho, O. *et al.* Adverse long-term effects of brain radiotherapy in adult low-grade glioma patients. *Neurology* **56**, 1285–1290 (2001).
3. Roman, D.D. & Sperduto, P.W. Neuropsychological effects of cranial radiation: Current knowledge and future directions. *Int. J. Radiat. Oncol. Biol. Phys.* **31**, 983–998 (1995).
4. Crossen, J.R., Garwood, D., Glatstein, E. & Neuwelt, E.A. Neurobehavioral sequelae of cranial irradiation in adults: A review of radiation-induced encephalopathy. *J. Clin. Oncol.* **12**, 627–642 (1994).
5. Abayomi, O.K. Pathogenesis of irradiation-induced cognitive dysfunction. *Acta Oncol.* **35**, 659–663 (1996).
6. Lee, P.W., Hung, B.K., Woo, E.K., Tai, P.T. & Choi, D.T. Effects of radiation therapy on neuropsychological functioning in patients with nasopharyngeal carcinoma. *J. Neurol. Neurosurg. Psychiatry* **52**, 488–492 (1989).

7. Hodges, H. *et al.* Late behavioural and neuropathological effects of local brain irradiation in the rat. *Behav. Brain Res.* **91**, 99–114 (1998).

8. Sienkiewicz, Z.J., Haylock, R.G. & Saunders, R.D. Prenatal irradiation and spatial memory in mice: Investigation of dose-response relationship. *Int. J. Radiat. Biol.* **65**, 611–618 (1994).

9. Tada, E., Parent, J.M., Lowenstein, D.H. & Fike, J.R. X-irradiation causes a prolonged reduction in cell proliferation in the dentate gyrus of adult rats. *Neuroscience* **99**, 33–41 (2000).

10. Peissner, W., Kocher, M., Treuer, H. & Gillardon, F. Ionizing radiation-induced apoptosis of proliferating stem cells in the dentate gyrus of the adult rat hippocampus. *Brain Res. Mol. Brain Res.* **71**, 61–68 (1999).

11. Parent, J.M., Tada, E., Fike, J.R. & Lowenstein, D.H. Inhibition of dentate granule cell neurogenesis with brain irradiation does not prevent seizure-induced mossy fiber synaptic reorganization in the rat. *J. Neurosci.* **19**, 4508–4519 (1999).

12. Snyder, J.S., Kee, N. & Wojtowicz, J.M. Effects of adult neurogenesis on synaptic plasticity in the rat dentate gyrus. *J. Neurophysiol.* **85**, 2423–2431 (2001).

13. Kempermann, G., Kuhn, H.G. & Gage, F.H. More hippocampal neurons in adult mice living in an enriched environment. *Nature* **386**, 493–495 (1997).

14. Gould, E., Beylin, A., Tanapat, P., Reeves, A. & Shors, T.J. Learning enhances adult neurogenesis in the hippocampal formation. *Nature Neurosci.* **2**, 260–265 (1999).

15. Shors, T.J. *et al.* Neurogenesis in the adult is involved in the formation of trace memories. *Nature* **410**, 372–376 (2001).

16. Dawirs, R.R., Hildebrandt, K. & Teuchert-Noodt, G. Adult treatment with haloperidol increases dentate granule cell proliferation in the gerbil hippocampus. *J. Neural Transm.* **105**, 317–327 (1998).

17. Leventhal, C., Rafii, S., Rafii, D., Shahar, A. & Goldman, S.A. Endothelial trophic support of neuronal production and recruitment from the adult mammalian subependyma. *Mol. Cell Neurosci.* **13**, 450–464 (1999).

18. Vallieres, L., Campbell, I.L., Gage, F.H. & Sawchenko, P.E. Reduced hippocampal neurogenesis in adult transgenic mice with chronic astrocytic production of interleukin-6. *J. Neurosci.* **22**, 486–492 (2002).

19. Calvo, W., Hopewell, J.W., Reinhold, H.S. & Yeung, T.K. Time- and dose-related changes in the white matter of the rat brain after single doses of X rays. *Br. J. Radiol.* **61**, 1043–1052 (1988).

20. Sheline, G.E., Wara, W.M. & Smith, V. Therapeutic irradiation and brain injury. *Int. J. Radiat. Oncol. Biol. Phys.* **6**, 1215–1228 (1980).

21. Pezner, R.D. & Archambeau, J.O. Brain tolerance unit: A method to estimate risk of radiation brain injury for various dose schedules. *Int. J. Radiat. Oncol. Biol. Phys.* **7**, 397–402 (1981).

22. Marks, J.E., Baglan, R.J., Prassad, S.C. & Blank, W.F. Cerebral radionecrosis: Incidence and risk in relation to dose, time, fractionation and volume. *Int. J. Radiat. Oncol. Biol. Phys.* **7**, 243–252 (1981).

23. Palmer, T.D., Willhoite, A.R. & Gage, F.H. Vascular niche for adult hippocampal neurogenesis. *J. Comp Neurol.* **425**, 479–494 (2000).

24. Gundersen, H.J. *et al.* The new stereological tools: Dissector, fractionator, nucleator and point sampled intercepts and their use in pathological research and diagnosis. *APMIS* **96**, 857–881 (1988).

25. Kuhn, H.G., Dickinson-Anson, H. & Gage, F.H. Neurogenesis in the dentate gyrus of the adult rat: Age-related decrease of neuronal progenitor proliferation. *J. Neurosci.* **16**, 2027–2033 (1996).

26. Gage, F.H. *et al.* Survival and differentiation of adult neuronal progenitor cells transplanted to the adult brain. *Proc. Natl. Acad. Sci. USA* **92**, 11879–11883 (1995).

27. Suhonen, J.O., Peterson, D.A., Ray, J. & Gage, F.H. Differentiation of adult hippocampus-derived progenitors into olfactory neurons *in vivo*. *Nature* **383**, 624–627 (1996).

28. Hong, J.H. *et al.* Induction of acute phase gene expression by brain irradiation. *Int. J. Radiat. Oncol. Biol. Phys.* **33**, 619–626 (1995).

29. Heyser, C.J., Masliah, E., Samimi, A., Campbell, I.L. & Gold, L.H. Progressive decline in avoidance learning paralleled by inflammatory neurodegeneration in transgenic mice expressing interleukin 6 in the brain. *Proc. Natl. Acad. Sci. USA* **94**, 1500–1505 (1997).

30. Louissaint, A., Rao, S., Leventhal, C. & Goldman, S.A. Coordinated interaction of neurogenesis and angiogenesis in the adult songbird brain. *Neuron* **34**, 945–960 (2002).

31. Lim, D.A. *et al.* Noggin antagonizes BMP signaling to create a niche for adult neurogenesis. *Neuron* **28**, 713–726 (2000).

32. Seaberg, R.M. & van der Kooy, D. Adult rodent neurogenic regions: the ventricular subependyma contains neural stem cells, but the dentate gyrus contains restricted progenitors. *J. Neurosci.* **22**, 1784–1793 (2002).

Extreme Sensitivity of Adult Neurogenesis to Low Doses of X-Irradiation[1]

Shinichiro Mizumatsu, Michelle L. Monje, Duncan R. Morhardt, Radoslaw Rola, Theo D. Palmer, and John R. Fike[2]

Brain Tumor Research Center, Department of Neurological Surgery, University of California at San Francisco, San Francisco, California 94143 [S. M., D. R. M., R. R., J. R. F.], and Department of Neurosurgery, Stanford University, Stanford, California 94305 [M. L. M., T. D. P.]

ABSTRACT

Therapeutic irradiation of the brain is associated with a number of adverse effects, including cognitive impairment. Although the pathogenesis of radiation-induced cognitive injury is unknown, it may involve loss of neural precursor cells from the subgranular zone (SGZ) of the hippocampal dentate gyrus and alterations in new cell production (neurogenesis). Young adult male C57BL mice received whole brain irradiation, and 6–48 h later, hippocampal tissue was assessed using immunohistochemistry for detection of apoptosis and numbers of proliferating cells and immature neurons. Apoptosis peaked 12 h after irradiation, and its extent was dose dependent. Forty-eight h after irradiation, proliferating SGZ cells were reduced by 93–96%; immature neurons were decreased from 40 to 60% in a dose-dependent fashion. To determine whether acute cell sensitivity translated into long-term changes, we quantified neurogenesis 2 months after irradiation with 0, 2, 5, or 10 Gy. Multiple injections of BrdUrd were given to label proliferating cells, and 3 weeks later, confocal microscopy was used to determine the percentage of BrdUrd-labeled cells that showed mature cell phenotypes. The production of new neurons was significantly reduced by X-rays; that change was dose dependent. In contrast, there were no apparent effects on the production of new astrocytes or oligodendrocytes. Measures of activated microglia indicated that changes in neurogenesis were associated with a significant inflammatory response. Given the known effects of radiation on cognitive function and the relationship between hippocampal neurogenesis and associated memory formation, our data suggest that precursor cell radiation response and altered neurogenesis may play a contributory if not causative role in radiation-induced cognitive impairment.

INTRODUCTION

Therapeutic irradiation of the brain can result in significant injury to normal brain structures. Although severe structural and functional injury generally occur after relatively high radiation doses (1–4), lower doses can lead to cognitive dysfunction without inducing significant morphological changes (5–10). Such cognitive changes can occur in both pediatric and adult patients and are often manifest as deficits in hippocampal-dependent functions of learning, memory, and spatial information processing (5, 7, 10–12).

Within the hippocampus, memory functions are associated with the principal cells of the hippocampal formation, *i.e.*, the pyramidal and granule cells of the dentate gyrus (13). New granule cells are produced from mitotically active neural precursor/stem cells in the SGZ;[3] this production of new cells occurs in all adult mammals, including humans (14–19). Newly born cells migrate into the GCL (20), develop granule cell morphology and neuronal markers (15), and connect with their target area, CA3 (21, 22). Recent studies show that

these new cells become functionally integrated into the dentate gyrus and have passive membrane properties, action potentials, and functional synaptic inputs similar to those found in mature dentate granule cells (23). Most importantly, the new neurons play a significant role in synaptic plasticity (24), which can be considered as a cellular substrate for learning. Furthermore, reductions in the number of newly generated neurons using the toxin methylazoxymethanal acetate impair learning (25), and recently, investigators using a hippocampal slice model showed that radiation-induced reductions in dentate neurogenesis were associated with an inhibition of long-term potentiation, a type of synaptic plasticity (26). Thus, any agent that damages neuronal precursor cells or their progeny, such as ionizing irradiation, could have a significant impact on neurogenesis and ultimately on specific cognitive functions associated with the hippocampus.

We (27–29) and others (30–32) have addressed the radiation response of cells in the dentate gyrus. In the rat, proliferating SGZ precursor cells undergo apoptosis after irradiation (27, 28), and reductions in precursor cell proliferation are still observed months after exposure (28). Furthermore, a single 10 Gy dose of X-rays to the rat brain almost completely abolishes the production of new neurons, whereas surviving precursor cells adopt a glial phenotype (29). Given the relationship between hippocampal neurogenesis and memory (19), and the significant effects of irradiation on SGZ precursor cells, it may be that radiation-induced impairment of SGZ neurogenesis plays a contributory if not causative role in the pathogenesis of cognitive dysfunction after irradiation. In the current study, we were interested in determining if there was a dose response relationship in terms of radiation-induced alterations in neurogenesis and, secondly, if acute changes in the SGZ were predictive of later developing changes in neurogenesis. Understanding how irradiation affects neurogenesis may provide useful insight into potential approaches/strategies to reduce cognitive impairment after cranial irradiation.

MATERIALS AND METHODS

Two-month-old male C57BL/J6 mice (~20 grams) were used in all studies. Mice were purchased from a commercial vendor (The Jackson Laboratory, Bar Harbor, ME) and housed and cared for in accordance with the United States Department of Health and Human Services Guide for the Care and Use of Laboratory Animals; all protocols were approved by the institutional Committee for Animal Research. Mice were kept in a temperature and light-controlled environment with a 12/12-h light/dark cycle and provided food and water *ad libitum*. All mice were anesthetized for irradiation and perfusion procedures; anesthesia consisted of an i.p. injection of ketamine (60 mg/kg) and a s.c. injection of medetomidine (0.25 mg/kg). Sham-irradiated mice were anesthetized as described.

Irradiation was done using a Phillips orthovoltage X-ray system as described previously (28, 33). Briefly, a special positioning jig was used so 4 animals could be irradiated simultaneously; the heads were centered in a 5×6 cm treatment field. The beam was directed down onto the head, and the body was shielded with lead. Dosimetry was done using a Keithley electrometer ionization chamber calibrated using lithium fluoride thermal luminescent dosimeters. The corrected dose rate was ~175 cGy/min at a source to skin distance of 21 cm.

Acute Radiation Response. To determine the time of peak apoptosis in the SGZ, groups of mice were irradiated with a single 10-Gy dose, and tissues were collected from 6 to 48 h later. Four sham-irradiated mice were killed at the time of irradiation. For determination of the radiation dose response for

[3] The abbreviations used are: SGZ, subgranular zone; GCL, granule cell layer; BrdUrd, 5-bromo-2'deoxyuridine; TUNEL, terminal deoxynucleotidyl transferase-mediated dUTP-biotin nick end labeling; Dcx, Doublecortin; NeuN, neuron-specific nuclear protein; ABC, avidin-biotinylated peroxidase complex; GFAP, glial fibrillary acidic protein; DAB, 3,3'-diaminobenzidine.

SGZ apoptosis, whole brain doses of 0, 1, 2, 5, and 10 Gy were given to groups of mice, and tissue was collected at the time of peak apoptosis; sham-irradiated mice were also killed at the time of peak apoptosis. To determine how radiation affected the cellular composition of the SGZ at a time when apoptosis was complete, groups of mice were irradiated with doses of 0, 2, 5, and 10 Gy, and tissues were collected 48 h later.

Mice were reanesthetized for tissue collection, and 50 ml of a 10% buffered formalin solution were infused into the ascending aorta using a mechanical pump (Masterflex Model 7014; Cole Parmer, Chicago, IL). After 5 min, mice were decapitated, and the brain was removed and immersed in a 10% buffered formalin solution for 3 days; tissue was stored in 70% ethanol until gross sectioning and paraffin embedding as described previously (28). A rotary microtome was used to cut 6-μm-thick transverse sections that were placed on polylysine-coated glass microscope slides.
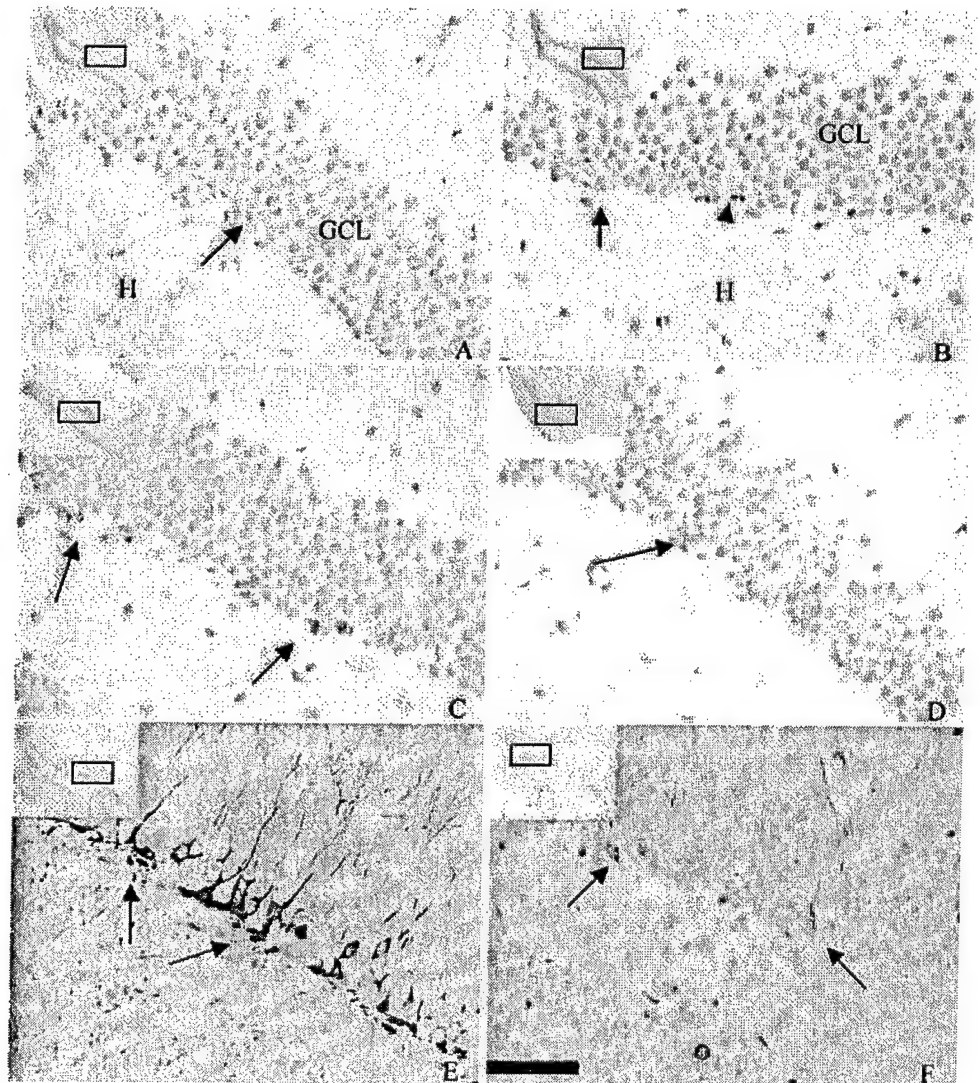
In the SGZ, apoptosis is characterized by cells showing morphological changes and/or TUNEL staining (28); only rarely does a given cell show both characteristics. Therefore, to get an estimate of the total number of apoptotic cells at a given time, both criteria were used in the present study. TUNEL-positive cells appeared as highly stained brown nuclei against the hematoxylin counterstain (Fig. 1, A and B). For the TUNEL procedure, all reagents were part of a kit (Apotag; Serological Corp., Norcross, GA), and the procedures were carried out as described previously (28, 34). Morphological changes included fragmentation, or the compaction of chromatin into two or more dense, lobulated masses, and pyknosis, which was characterized by small, round, darkly staining nuclei. To minimize the impact of including any normal cell profiles (*i.e.*, glia) in our counts of apoptosis, if any cytoplasm was

observed in conjunction with a small, dense nucleus, that cell was not considered as apoptotic.

To determine radiation-induced changes in the cellular composition of the SGZ, proliferating cells were labeled with an antibody against Ki-67, a nuclear antigen that is expressed during all stages of the cell cycle except G_0 (35, 36). Immature neurons were detected using an antibody against Dcx, the predicted gene product of the *XLIS* gene (37) that is associated with neuronal or neuroblast migration (37–39). For all immunostaining, binding of biotinylated secondary antibodies was detected using an ABC system (Vector, Burlingame, CA). To quench endogenous peroxidase activity, deparaffinized specimens were soaked for 30 min in 0.3% H_2O_2 (Sigma, St. Louis, MO) in 70% ethanol. After the primary and secondary antibodies were applied, the specimens were incubated with the ABC reagent for 30 min and developed with 0.025% DAB (Sigma) dissolved in double distilled water containing 0.005% H_2O_2. Sections were then counterstained with Gill's hematoxylin, dehydrated, and mounted.

Ki67. After deparaffinization and quenching of endogenous peroxidase, tissue sections were soaked in 10 mM sodium citrate buffer (pH 6.0) and boiled for 10 min using a microwave oven. Sections were left in the citrate buffer for another 20 min, washed in PBS, and then incubated with 2% normal rabbit serum for 30 min. Sections were incubated overnight at 4°C with primary antibody (DakoCytomation, Carpinteria, CA) diluted 1:100 in PBS with 2% normal rabbit serum. After washing, sections were incubated for 30 min at room temperature with biotin-conjugated rabbit antirat IgG (Vector) diluted 1:200 in PBS with 2% normal rabbit serum. Finally, the specimens were incubated with ABC reagent, developed with DAB, and counterstained.

Fig. 1. Photomicrographs depicting specific cellular responses in mouse dentate gyrus before irradiation (A, C, and E) and either 12 h (B) or 48 h after 10 Gy (D and E). *Panels* include apoptosis (A and B), proliferating cells (Ki-67, C, and D), and immature neurons (Dcx, E, and F). The SGZ is a narrow band of cells between the hilus (H) and GCL. Apoptotic nuclei are characterized by TUNEL labeling (*arrows* in A and B) or dense chromatin/nuclear fragmentation (*arrowhead, B*). Although an occasional apoptotic nucleus was seen in tissues from unirradiated mice (A), a significant increase in apoptosis was seen in the SGZ 12 h after irradiation (B). Proliferating Ki-67-positive cells (*arrows, C*) are spread out within the SGZ in tissues from unirradiated animals; only an occasional Ki-67-positive cell was found after 10 Gy (D). Dcx-positive cells are highly concentrated in the SGZ and lower regions of the GCL of unirradiated mice (*arrows, E*). After 10 Gy, there are substantially fewer Dcx-positive cells (F). All micrographs are ×40; the scale bar in F represents 50 μm. The *inset* in each *panel* is a low power image (×10) of the dentate gyrus; *black boxes,* the areas photographed at ×40.
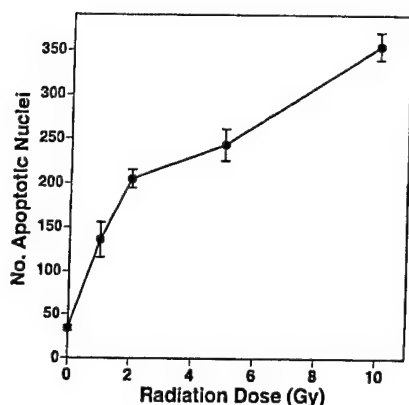
Fig. 2. Cells in the dentate SGZ undergo dose-dependent apoptosis after low to moderate doses of X-rays. Apoptosis was quantified based on TUNEL labeling and morphological changes in irradiated cells. The steepest part of the response was dominated by loss of actively proliferating cells, whereas the shallower slope, >2 Gy, largely represented the response of immature neurons. Each datum point represents a mean of 4–7 mice; error bars, SE.

Dcx. After deparaffinization and quenching, sections were microwave treated in citrate buffer as described above. After washing with PBS and blocking for 30 min using 5% normal horse serum, sections were incubated overnight at 4°C with primary antibody (Santa Cruz Biotechnology, Santa Cruz, CA) diluted 1:500 in PBS with 5% normal horse serum. Sections were washed and incubated for 60 min at room temperature in biotinylated antigoat IgG (Vector) diluted 1:500 in 5% normal horse serum. Sections were finally incubated with ABC reagent, developed with DAB, and counterstained.

The number of cells showing specific characteristics of apoptosis, along with the numbers of proliferating cells and immature neurons, were scored blind using a histomorphometric approach (27, 28, 34). A standardized counting area was used that involved 6-μm-thick coronal sections from three different brain levels representing the rostral/mid hippocampus (27, 28). The brain levels were ~50 μm apart, and the most rostral brain level corresponded to a point ~2.5 mm behind the bregma. For each mouse, three nonoverlapping sections were analyzed, one each from the three regions of the hippocampus. Quantification was made of all positively labeled cells within the SGZ of the suprapyrimidal and infrapyrimidal blades of the dentate gyrus. The total number of positively labeled cells was determined by summing the values from both hemispheres in all three tissue sections.

Neurogenesis. To determine the effects of irradiation on the production of new cells in the SGZ (*i.e.*, neurogenesis), groups of mice were given whole brain doses of 0, 2, 5, or 10 Gy and allowed to recover from anesthesia. Four weeks after irradiation, each mouse received a single i.p. injection (50 mg/kg) of BrdUrd (Sigma) daily for 7 days. Three weeks after the last BrdUrd injection, mice were anesthetized and perfused with cold saline followed by cold 4% paraformaldehyde made up the day of perfusion. The brain was removed and postfixed in paraformaldehyde overnight and then equilibrated in phosphate-buffered 30% sucrose. Free floating 50-μm-thick sections were cut on a freezing microtome and stored in cryoprotectant. Sections were immunostained as described (29, 40) using the following primary antibodies and working concentrations: (*a*) rat anti-BrdUrd (1:10; Oxford Biotechnology, Kidlington, Oxford, United Kingdom); (*b*) mouse anti-NeuN (1:200; Chemicon, Temecula, CA); (*c*) rabbit anti-NG2 (1:200; Chemicon); (*d*) guinea pig anti-GFAP (1:800; Advanced Immunochemical, Inc., Long Beach, CA); and (*e*) rat anti-CD68 (FA11; 1:20; Serotec, Inc., Raleigh, NC).

Confocal microscopy was performed using a Zeiss 510 confocal microscope (Thornwood, NY), using techniques described previously (29, 40). The primary confocal end point was the proportion of BrdUrd-positive cells that coexpressed each lineage-specific phenotype. Cell counts were limited to the dentate GCL and a 50-μm border along the hilar margin that included the SGZ. When possible, ~100 BrdUrd-positive cells were scored for each marker per animal. Each cell was manually examined in its full "z" dimension, and only those cells for which the BrdUrd-positive nucleus was unambiguously associated with the lineage-specific marker were scored as positive.

Statistics. For immunohistochemical end points, values for all animals in a given treatment group were averaged, and SE were calculated. A two-sided

Jonckhere-Terpstra test was used to determine whether cellular changes in radiation response were monotonic, *i.e.*, either increasing or decreasing with increasing treatment dose.

RESULTS

The SGZ is an area of active cell proliferation in young adult mice, and proliferating Ki-67-positive cells occur along both blades of the dentate gyrus (Fig. 1*C*). Proliferating cells were observed occasionally in the hilus, but no Ki-67-positive cells were observed in the dentate GCL. In our standardized counting area, the number of Ki-67-positive cells averaged 137.2 ± 7 (*n* = 7) in sham-irradiated mice. Immature neurons (Dcx positive) were observed in large numbers in the SGZ (Fig. 1*E*), averaging 480.3 ± 19.9 (*n* = 4) in sham-irradiated animals. Dcx-positive cells were also observed in the GCL, averaging 135.8 ± 9.6 (*n* = 4) in the first 25 μm from the SGZ, 27.3 ± 3.1 in the next 25 μm, and 2 ± 0.8 in the rest of the GCL.

In sham-irradiated mice from our dose response study, the total number of apoptotic nuclei in our standardized counting area averaged 33.8 ± 2.9 (*n* = 5); apoptotic nuclei occurred in both blades of the dentate gyrus and usually appeared alone. Apoptotic nuclei were observed in the GCL of sham-irradiated mice rarely, and only an occasional apoptotic body was observed in the hilus. After irradiation, apoptotic nuclei occurred singly or in small groups and were detected in the SGZ of both blades of the dentate gyrus (Fig. 1*B*). Apoptotic nuclei were seen in the GCL and hilus after irradiation but at much lower levels than in the SGZ. On the basis of morphological identification of the microvasculature, there were few apoptotic endothelial cells seen after irradiation.

The time course for SGZ apoptosis was determined to select a time for tissue collection in our dose response study. Six h after irradiation, the number of apoptotic nuclei was not substantially different from that seen in sham-irradiated mice; apoptosis peaked 12 h after irradiation and then decreased to near control levels by 48 h (data not shown). The dose response curve for SGZ apoptosis was then determined at the time of peak apoptosis, 12 h after irradiation. There was a significant increase in apoptosis with radiation dose (*P* < 0.001), and the dose response curve had two components: (*a*) a steep portion from 0 to 2 Gy; and (*b*) a shallower slope after higher doses (Fig. 2). Relative to sham-irradiated controls, the numbers of proliferating cells observed at 12 h were reduced (Fig. 1*D*) by 75% after 1 Gy and ~90% after doses of 2–10 Gy. At that time, the numbers of immature neurons in the SGZ were reduced (Fig. 1*F*) by 36, 51, 56, and 67% after 1, 2, 5, and 10 Gy, respectively.

To estimate the full acute impact of irradiation on the SGZ, we

Fig. 3. Numbers of proliferating cells (*left panel*) and immature neurons (*right panel*) in the dentate SGZ are significantly decreased 48 h after irradiation. Antibodies against Ki-67 and Dcx were used to detect proliferating cells and immature neurons, respectively. All doses substantially reduced the numbers of proliferating cells, and the dose response from 2 to 10 Gy was significant (*P* < 0.05). Immature neurons were also reduced in a dose-dependent fashion (*P* < 0.001). Each bar represents an average of 4 animals; error bars, SE.

Fig. 4. Two months after irradiation, cell fate in the dentate gyrus is altered by low to moderate doses of X-rays. Confocal images (*top*) were used to quantify the percentage of BrdUrd-positive cells that coexpressed mature cell markers. Proliferating cells were labeled with BrdUrd (*red/orange* stain in confocal images), and 3 weeks later, the relative prop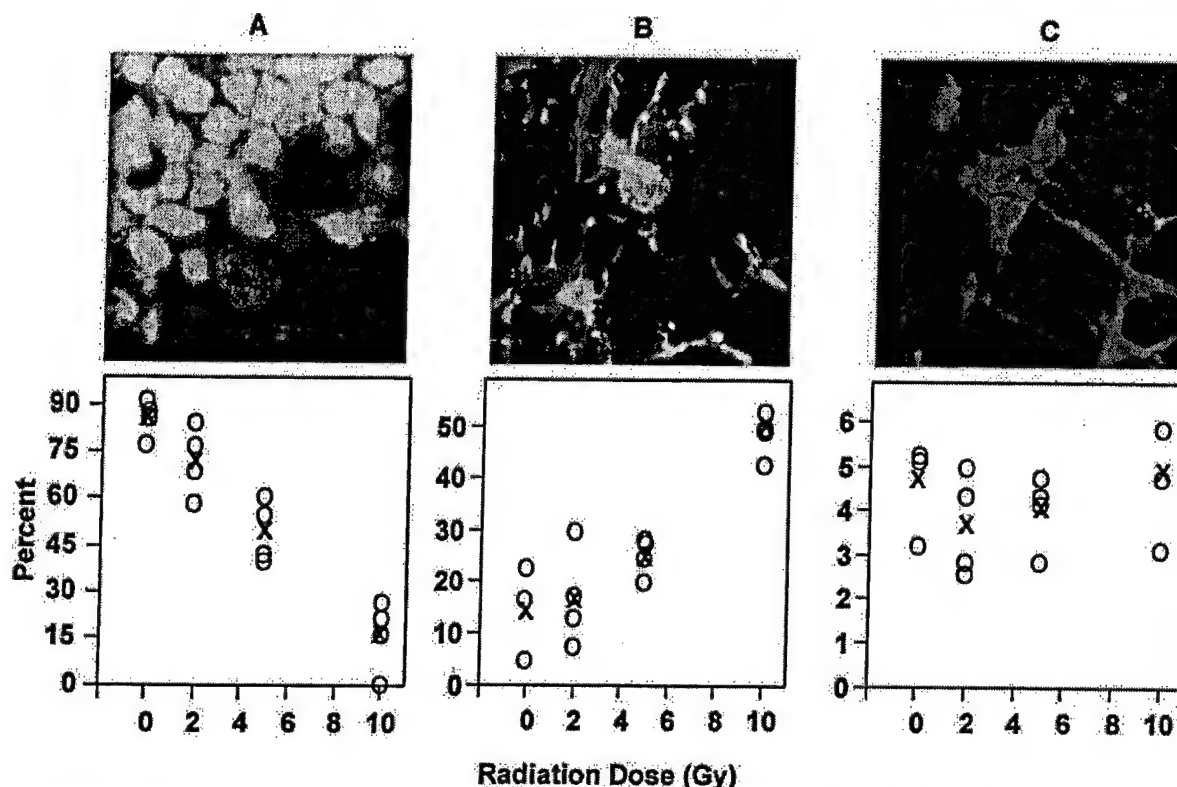ortion of cells adopting a recognized cell fate was determined as a function of radiation dose (*bottom*). Neurons (*green* cells in *A, top*), oligodendrocytes (*green* cells in *B, top*), and astrocytes (*blue* cells in *C, top*) were labeled with antibodies against NeuN, NG2, and GFAP, respectively. Each of the confocal images shows a double-labeled cell. The production of new neurons (*A, bottom*) was reduced in a dose-dependent fashion ($P < 0.001$), whereas there was no apparent change in the production of GFAP with dose (*C, bottom*). In contrast, the percentage of BrdUrd-positive cells adopting an oligodendrocyte fate (*B, bottom*) appeared to increase, particularly after 10 Gy. In the graphs, each *circle* represents the value from an individual animal; each *X* represents the mean value for a given dose group.

quantified the numbers of proliferating cells and immature neurons remaining after apoptosis was complete. Forty-eight h after exposure, there was a substantial reduction in the number of proliferating cells (Fig. 3); the dose response in Ki-67 labeling from 2 to 10 Gy was significant ($P < 0.05$). Dcx-positive cells were reduced by all doses, and the dose response relationship was highly significant ($P < 0.001$; Fig. 3). Because immature neurons generally move into the GCL as they differentiate, we quantified the numbers of Dcx-positive cells in the GCL to determine whether the sensitivity of immature neurons changed as they moved away from the SGZ. In the SGZ, the percentage decrease in cell number relative to controls was 41, 53, and 61% in the SGZ after 2, 5, and 10 Gy. The numbers of Dcx-positive cells in the GCL were decreased ~19.8, 26, and 52.7% after 2, 5, and 10 Gy, respectively.

To determine the fate of new cells produced by surviving precursor cells, we gave multiple injections of BrdUrd and 3 weeks later used cell-specific antibodies to assess the phenotype of BrdUrd-positive cells. Overall, BrdUrd labeling was reduced by all of the doses used here, with 2 and 5 Gy reducing the number of BrdUrd-positive cells by 40–50% and 10 Gy by ~75%. In sham-irradiated controls, 85.3 ± 5.1% ($n = 4$) of BrdUrd-positive cells coexpressed the neuronal marker NeuN. After irradiation, there was a significant dose-dependent decrease in the percentage of BrdUrd-positive cells coexpressing NeuN ($P < 0.001$; Fig. 4A), and after the highest dose used here (10 Gy), the fraction of double-labeled cells was ~19% of control.

In contrast to our results for new neuron production, there was no apparent effect of irradiation on the percentage of BrdUrd-labeled cells that coexpressed GFAP (Fig. 4C). With respect to newly pro-

duced immature oligodendrocytes, there appeared to be a significant ($P < 0.001$) dose-related increase in the percentage of BrdUrd-labeled cells colabeling with NG2; however, that increase was dominated by the response seen after 10 Gy (Fig. 4B). Subsequent studies by us indicated that after 10 Gy, many BrdUrd-NG2 double-labeled cells also colabeled with the monocyte marker CD11B and represent infiltrating peripheral monocytes.[4]

On the basis of our earlier rat study showing that decreased neurogenesis after irradiation was attributable in part to an altered microenvironment (29), we were interested in determining if the dose-related changes we observed in neurogenesis were accompanied by changes in the local inflammatory response. Forty-eight h after 10 Gy, there were no activated microglia detected in or around the SGZ (data not shown). However, there was a significant dose-related increase in the number of activated microglia ($P < 0.001$) observed 2 months after irradiation (Fig. 5).

DISCUSSION

The main findings of the present study are: (*a*) cells of the dentate SGZ are extremely sensitive to X-rays; (*b*) hippocampal neurogenesis is altered by irradiation with the production of new neurons decreasing as a function of radiation dose; (*c*) a dose-dependent inflammatory reaction occurs in conjunction with altered neurogenesis; and (*d*) acute dose-related changes in SGZ precursor cells qualitatively cor-

---

[4] M. L. Monje and T. D. Palmer, unpublished observations.

[5] J. Raber, R. Rola, A. LeFevour, D. R. Morhardt, J. Curley, S. Mizumatsu, and J. R. Fike. Radiation-induced cognitive impairments are associated with changes in hippocampal neurogenesis, submitted for publication.
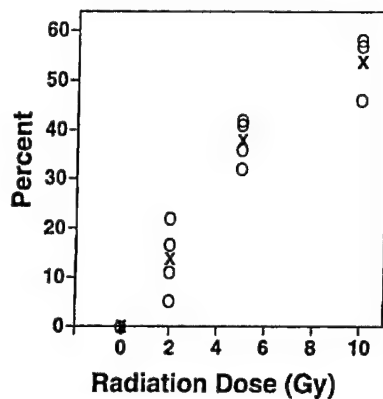
Fig. 5. Two months after irradiation, there is a substantial inflammatory response in the dentate SGZ. Proliferating cells were first labeled with BrdUrd, and 3 weeks later, the relative proportion of cells (*Percent*) adopting a microglial phenotype was determined as a function of radiation dose. Activated microglia were detected using an antibody against CD68. There were no activated microglia detected in unirradiated controls (*D*), but there was a significant ($P < 0.001$) dose-related increase in activated microglia after irradiation. Each *circle* represents the value from an individual animal; each *X* represents the mean value for a given dose group.

relate with later decreases in new neuron production. Given the potential of ionizing irradiation to induce significant cognitive effects in adults and children undergoing radiotherapy, and the role of the hippocampus in specific cognitive functions, our findings support the idea that changes in SGZ neurogenesis may play an important role in radiation-induced cognitive impairment.

The effects of ionizing irradiation on hippocampal structure and function have been addressed primarily in prenatal or neonatal animals (41–46) but also in adults (47–49). Although some investigators have proposed a link between radiation-induced hippocampal damage and cognitive deficits, it was not until recently that it was suggested that changes in the neural precursor population in the hippocampus might be involved (28, 29). Studies in rats (28, 31) indicated that proliferating SGZ cells were particularly sensitive to irradiation, a finding confirmed here in mice at both 12 and 48 h (Fig. 3) after irradiation. Our results, showing that ~90% of Ki-67-positive cells were already gone at the time of peak apoptosis, independent of dose > 1 Gy, suggested that the steep portion of the apoptosis dose response curve (Fig. 2) primarily reflected the response of actively proliferating cells. Given that the number of apoptotic nuclei measured here represented only a snapshot in time, the numbers of dying cells seen at 12 h far surpassed the number of proliferating cells in our standardized counting area. This difference was largely accounted for by the significant reduction in the number of immature neurons. The dose response relationship for Dcx-positive cells seen both 12 and 48 h (Fig. 3) after irradiation indicated that the death of immature neurons likely dominated the apoptosis dose response curve from 2 to 10 Gy. Thus, radiation not only affected the input of new cells in the SGZ (*i.e.*, proliferating Ki-67-positive cells) but also early differentiating neurons, and those effects were dose dependent. Our finding that irradiation affected Dcx-positive cells in the SGZ zone to a greater extent than those that had migrated into the GCL suggested that as cells migrated further away from the SGZ, they became less sensitive to irradiation. Whether this response represented different environmental factors or simply the fact that the cells were becoming more differentiated is not yet clear.

The process of neurogenesis consists of distinct developmental processes, including proliferation, survival, and differentiation (50). Many investigators use only proliferation as an indicator of neurogenesis, and immunostaining for BrdUrd is a well-established technique to detect cells in the S phase of the cell cycle. However, to measure migration and differentiation, post-BrdUrd survival time has

to be long enough to allow newly born cells to move away and begin to express mature cell markers. Our BrdUrd-labeling paradigm in conjunction with immunochemistry and confocal microscopy facilitated our assessment of all three criteria of neurogenesis. In our study, there was a clear dose response with respect to the percentage of BrdUrd-labeled cells that coexpressed neuron-specific NeuN; after 10 Gy, the reduction was 81% relative to sham-irradiated controls. In rats, a similar dose almost completely ablated neuronal production (29). Although this difference is probably species dependent, in both cases, there was a clear impact of X-rays on the production of new neurons, and in the present study, the impact was dose dependent and occurred after clinically relevant doses, *i.e.*, 2–5 Gy. Although the production of new neurons was substantially reduced relative to control, glial cell fate was unchanged by irradiation (astrocytes) or appeared to increase (immature oligodendrocytes). The relative increase in the percentage of cells adopting an oligodendrocyte phenotype was high relative to control but only after 10 Gy (Fig. 4). However, recent studies in rats show that after 10 Gy, about half of the cells double labeled with BrdUrd and NG2 are infiltrating monocytes.[4] This agrees with recently published work that showed that after central nervous system injury, infiltrating monocytes were immunoreactive for the anti-NG2 antibody used here (51, 52). Thus, it is likely that the increase in immature oligodendrocytes seen here (Fig. 4*B*) did not really reflect the production of new oligodendrocytes but rather was a manifestation of a postirradiation inflammatory response. This is consistent with our previous work in rats (29) that showed that after irradiation, gliogenesis was relatively preserved compared with the production of new neurons. Whether this represents a relative resistance of glial progenitor cells, an aberrant regulation of differentiation, or alterations in the microenvironment that could adversely affect fate decisions is not known. Whatever the mechanism(s) involved, our data clearly showed that the production of new neurons was more sensitive to low doses of irradiation than the production of glia.

Neurogenesis depends on a complex microenvironment that involves signaling between multiple cell types, and irradiation could affect any or all of these cells or interactions (29). Although the precise nature of such effects has not yet been clarified, chronic inflammatory changes and disturbance of the normal association between precursor cells and the microvasculature have been suggested (29). We did not specifically address the microvasculature in this study, but we did see significant differences between irradiated animals and controls in the numbers of activated microglia (Fig. 5). Although our data indicated that activated microglia did not seem to be associated with the acute losses of proliferating cells and immature neurons, they did appear to be temporally related to changes in neurogenesis. Given the potential role of proinflammatory cytokines in radiation brain injury (53–55), and the impact of specific cytokines on neurogenesis (56), it is possible that the activation of microglia may constitute a critical factor in the radiation-induced depression of neuron production.

Low to moderate single doses of X-rays clearly induced early dose-related changes in the mouse SGZ, and cell proliferation was still reduced months after irradiation. Furthermore, although some proliferation still took place after irradiation, there were significant reductions in the production of new neurons. Although acute and later-developing changes in the SGZ were both dose dependent, there are some uncertainties about the relationship between these effects. Our earlier study in rats suggested that acute radiation toxicity in the SGZ primarily affected rapidly expanding yet committed precursor cell populations (29), and the present studies support that idea. However, later effects may involve another population: relatively quiescent stem/precursor cells that appear to be responsible for repopulating a

damaged SGZ (57). A loss of such a population could result in changes that are slower in evolving and that are dose dependent; our neurogenesis data constitute such a finding. Clearly, the relationships between acute and later-developing effects are complex, and the mechanism(s) linking cell loss, reduced neurogenesis, and other factors, such as inflammation, need to be determined.

Given the apparent relationship between hippocampal neurogenesis and associated memory formation (19), the responses seen here may have an important impact in our understanding of radiation-induced cognitive impairment. Although the present data do not directly link altered neurogenesis with cognitive function, in a separate study, we have been able to show that 3 months after a single dose of 10 Gy, there is a persistent and significant decrease in the numbers of proliferating cells and immature neurons in the SGZ and a concomitant impairment of hippocampal-dependent cognitive function.[5] Although a cause-and-effect relationship has yet to be shown, the present data along with our unpublished cognitive studies are highly suggestive that there is a link between radiation-induced depression of neuron production and subsequent functional impairment. If true, and given the various factors that influence neurogenesis (24, 58–60), it may be possible to ameliorate or rescue individuals at risk for cognitive dysfunction after therapeutic irradiation involving the brain.

ACKNOWLEDGMENTS

REFERENCES

1. Fike, J. R., and Gobbel, G. T. Central nervous system radiation injury in large animal models. *In:* P. H. Gutin, S. A. Leibel, and G. E. Sheline (eds.), Radiation Injury to the Nervous System, pp. 113–135. New York: Raven Press, Ltd., 1991.
2. Hopewell, J. W. Late radiation damage to the central nervous system: a radiological interpretation. Neuropathol. Appl. Neurobiol., *5:* 329–343, 1979.
3. Sheline, G. E., Wara, W. M., and Smith, V. Therapeutic irradiation and brain injury. Int. J. Radiat. Oncol. Biol. Phys., *6:* 1215–1228, 1980.
4. Tofilon, P. J., and Fike, J. R. The radioresponse of the central nervous system: a dynamic process. Radiat. Res., *153:* 357–370, 2000.
5. Abayomi, O. K. Pathogenesis of irradiation-induced cognitive dysfunction. Acta Oncol., *35:* 659–663, 1996.
6. Butler, R. W., Hill, J. M., Steinherz, P. G., Meyers, P. A., and Finlay, J. L. Neuropsychologic effects of cranial irradiation, intrathecal methotrexate, and systemic methotrexate in childhood cancer. J. Clin. Oncol., *12:* 2621–2629, 1994.
7. Crossen, J. R., Garwood, D., Glatstein, E., and Neuwelt, E. A. Neurobehavioral sequelae of cranial irradiation in adults: a review of radiation-induced encephalopathy. J. Clin. Oncol., *12:* 627–642, 1994.
8. Dennis, M., Spiegler, B. J., Obonsawin, M. C., Maria, B. L., Cowell, C., Hoffman, H. J., Hendrick, E. B., Humphreys, R. P., Bailey, J. D., and Ehrlich, R. M. Brain tumors in children and adolescents-III. Effects of radiation and hormone status on intelligence and on working, associative and serial-order memory. Neuropsychologia, *30:* 257–275, 1992.
9. Kramer, J. H., Crittenden, M. R., Halberg, F. E., Wara, W. M., and Cowan, M. J. A prospective study of cognitive functioning following low-dose cranial radiation for bone marrow transplantation. Pediatrics, *90:* 447–450, 1992.
10. Roman, D. D., and Sperduto, P. W. Neuropsychological effects of cranial radiation: current knowledge and future directions. Int. J. Radiat. Oncol. Biol. Phys., *31:* 983–998, 1995.
11. Lee, P. W., Hung, B. K., Woo, E. K., Tai, P. T., and Choi, D. T. Effects of radiation therapy on neuropsychological functioning in patients with nasopharyngeal carcinoma. J. Neurol. Neurosurg. Psychiatry, *52:* 488–492, 1989.
12. Surma-aho, O., Niemela, M., Vilkki, J., Kouri, M., Brander, A., Salonen, O., Paetau, A., Kallio, M., Pyykkonen, J., and Jaaskelainen, J. Adverse long-term effects of brain radiotherapy in adult low-grade glioma patients. Neurology, *56:* 1285–1290, 2001.
13. Collier, T. J., Quirk, G. J., and Routtenberg, A. Separable roles of hippocampal granule and pyramidal cells in remembering spatial information. Brain Res., *409:* 316–328, 1987.
14. Bayer, S. A. Changes in the total number of dentate granule cells in juvenile and adult rats: a correlated volumetric and 3H-thymidine autoradiographic study. Exp. Brain Res., *46:* 315–323, 1982.
15. Cameron, H. A., Woolley, C. S., McEwen, B. S., and Gould, E. Differentiation of newly born neurons and glia in the dentate gyrus of the adult rat. Neuroscience, *56:* 337–344, 1993.
16. Gould, E., McEwen, B. S., Tanapat, P., Galea, L. A., and Fuchs, E. Neurogenesis in the dentate gyrus of the adult tree shrew is regulated by psychosocial stress and NMDA receptor activation. J. Neurosci., *17:* 2492–2498, 1997.
17. Kempermann, G., Kuhn, H. G., and Gage, F. H. More hippocampal neurons in adult mice living in an enriched environment. Nature (Lond.), *386:* 493–495, 1997.
18. Eriksson, P. S., Perfilieva, E., Bjork-Eriksson, T., Alborn, A. M., Nordborg, C., Peterson, D. A., and Gage, F. H. Neurogenesis in the adult human hippocampus. Nat. Med., *4:* 1313–1317, 1998.
19. Gould, E., Beylin, A., Tanapat, P., Reeves, A., and Shors, T. J. Learning enhances adult neurogenesis in the hippocampal formation. Nat. Neurosci., *2:* 260–265, 1999.
20. Kuhn, H. G., Dickinson-Anson, H., and Gage, F. H. Neurogenesis in the dentate gyrus of the adult rat: age-related decrease of neuronal progenitor proliferation. J. Neurosci., *16:* 2027–2033, 1996.
21. Stanfield, B. B., and Trice, J. E. Evidence that granule cells generated in the dentate gyrus of adult rats extend axonal projections. Exp. Brain Res., *73:* 399–406, 1988.
22. Markakis, E. A., and Gage, F. H. Adult-generated neurons in the dentate gyrus send axonal projections to field CA3 and are surrounded by synaptic vesicles. J. Comp. Neurol., *406:* 449–460, 1999.
23. van Praag, H., Schinder, A. F., Christie, B. R., Toni, N., Palmer, T. D., and Gage, F. H. Functional neurogenesis in the adult hippocampus. Nature (Lond.), *415:* 1030–1034, 2002.
24. van Praag, H., Christie, B. R., Sejnowski, T. J., and Gage, F. H. Running enhances neurogenesis, learning, and long-term potentiation in mice. Proc. Natl. Acad. Sci. USA, *96:* 13427–13431, 1999.
25. Shors, T. J., Miesegaes, G., Beylin, A., Zhao, M., Rydel, T., and Gould, E. Neurogenesis in the adult is involved in the formation of trace memories. Nature (Lond.), *410:* 372–376, 2001.
26. Snyder, J. S., Kee, N., and Wojtowicz, J. M. Effects of adult neurogenesis on synaptic plasticity in the rat dentate gyrus. J. Neurophysiol., *85:* 2423–2431, 2001.
27. Parent, J. M., Tada, E., Fike, J. R., and Lowenstein, D. H. Inhibition of dentate granuale cell neurogenesis with brain irradiation does not prevent seizure-induced mossy fiber synaptic reorganization in the rat. J. Neurosci., *19:* 4508–4519, 1999.
28. Tada, E., Parent, J. M., Lowenstein, D. H., and Fike, J. R. X-irradiation causes a prolonged reduction in cell proliferation in the dentate gyrus of adult rats. Neuroscience, *99:* 33–41, 2000.
29. Monje, M. L., Mizumatsu, S., Fike, J. R., and Palmer, T. D. Irradiation induces neural precursor-cell dysfunction. Nat. Med., *8:* 955–962, 2002.
30. Nagai, R., Tsunoda, S., Hori, Y., and Asada, H. Selective vulnerability to radiation in the hippocampal dentate granule cells. Surg. Neurol., *53:* 503–506; discussion 506–507, 2000.
31. Peissner, W., Kocher, M., Treuer, H., and Gillardon, F. Ionizing radiation-induced apoptosis of proliferating stem cells in the dentate gyrus of the adult rat hippocampus. Brain Res. Mol. Brain Res., *71:* 61–68, 1999.
32. Sasaki, R., Matsumoto, A., Itoh, K., Kawabe, T., Ota, Y., Yamada, K., Maruta, T., Soejima, T., and Sugimura, K. Target cells of apoptosis in the adult murine dentate gyrus and O4 immunoreactivity after ionizing radiation. Neurosci. Lett., *279:* 57–60, 2000.
33. Tada, E., Yang, C., Gobbel, G. T., Lamborn, K. R., and Fike, J. R. Long term impairment of subependymal repopulation following damage by ionizing irradiation. Exp. Neurol., *160:* 66–77, 1999.
34. Shinohara, C., Gobbel, G. T., Lamborn, K. R., Tada, E., and Fike, J. R. Apoptosis in the subependyma of young adult rats after single and fractionated doses of x-rays. Cancer Res., *57:* 2694–2702, 1997.
35. Fisher, B. J., Naumova, E., Leighton, C. C., Naumov, G. N., Kerklviet, N., Fortin, D., Macdonald, D. R., Cairncross, J. G., Bauman, G. S., and Stitt, L. Ki-67: a prognostic factor for low-grade glioma? Int. J. Radiat. Oncol. Biol. Phys., *2:* 996–1001, 2002.
36. Kee, N., Sivalingam, S., Boonstra, R., and Wojtowicz, J. M. The utility of Ki-67 and BrdU as proliferative markers of adult neurogenesis. J. Neurosci. Methods, *115:* 97–105, 2002.
37. Mizuguchi, M., Qin, J., Yamada, M., Ikeda, K., and Takashima, S. High expression of doublecortin and KIAA0369 protein in fetal brain suggests their specific role in neuronal migration. Am. J. Pathol., *155:* 1713–1721, 1999.
38. Nacher, J., Crespo, C., and McEwen, B. S. Doublecortin expression in the adult rat telencephalon. Eur. J. Neurosci., *14:* 629–644, 2001.
39. Englund, U., Bjorklund, A., and Wictorin, K. Migration patterns and phenotypic differentiation of long-term expanded human neural progenitor cells after transplantation into the adult rat brain. Brain Res. Dev. Brain Res., *134:* 123–141, 2002.
40. Palmer, T. D., Willhoite, A. R., and Gage, F. H. Vascular niche for adult hippocampal neurogenesis. J. Comp. Neurol., *425:* 479–494, 2000.
41. Czurko, A., Czeh, B., Seress, L., Nadel, L., and Bures, J. Severe spatial navigation deficit in the Morris water maze after single high dose of neonatal x-ray irradiation in the rat. Proc. Natl. Acad. Sci. USA, *94:* 2766–2771, 1997.
42. Mickley, G. A., Ferguson, J. L., Mulvihill, M. A., and Nemeth, T. J. Progressive behavioral changes during the maturation of rats with early radiation-induced hypoplasia of fascia dentata granule cells. Neurotoxicol. Teratol., *11:* 385–393, 1989.
43. Moreira, R. C. M., Moreira, M. V., Bueno, J. L. O., and Xavier, G. F. Hippocampal lesions induced by ionizing radiation: a parametric study. J. Neurosci. Methods, *75:* 41–47, 1997.
44. Sienkiewicz, Z. J., Haylock, R. G., and Saunders, R. D. Prenatal irradiation and spatial memory in mice: investigation of dose-response relationship. Int. J. Radiat. Biol., *65:* 611–618, 1994.
45. Sienkiewicz, Z. J., Saunders, R. D., and Butland, B. K. Prenatal irradiation and spatial memory in mice: investigation of critical period. Int. J. Radiat. Biol., *62:* 211–219, 1992.

46. Sienkiewicz, Z. J., Haylock, R. G., and Saunders, R. D. Differential learning impairments produced by prenatal exposure to ionizing radiation in mice. Int. J. Radiat. Biol., *75:* 121–127, 1999.

47. Akiyama, K., Tanaka, R., Sato, M., and Taked, N. Cognitive dysfunction and histological findings in adult rats one year after whole brain irradiation. Neurol. Med. Chir. (Tokyo), *41:* 590–598, 2001.

48. Hodges, J., Katzung, N., Sowinski, P., Hopewell, J. W., Wilkinson, J. H., Bywaters, T., and Rezvani, M. Late behavioral and neuropathological effects of local brain irradiation in the rat. Behav. Brain Res., *91:* 99–114, 1998.

49. Lamproglou, I., Chen, Q. M., Boisserie, G., Mazeron, J-J., Poisson, M., Baillet, F., Le Poncin, M., and Delattre, J-V. Radiation-induced cognitive dysfunction: an experimental model in the old rat. Int. J. Radiat. Oncol. Biol. Phys., *31:* 65–70, 1995.

50. Kempermann, G., Kuhn, H. G., and Gage, F. H. Experience-induced neurogenesis in the senescent dentate gyrus. J. Neurosci., *18:* 3206–3212, 1998.

51. Bu, J., Akhtar, N., and Nishiyama, A. Transient expression of the NG2 proteoglycan by a subpopulation of activated macrophages in an excitotoxic hippocampal lesion. Glia, *34:* 296–310, 2001.

52. Jones, L. L., Yamaguchi, Y., Stallcup, W. B., and Tuszynski, M. H. NG2 is a major chondroitin sulfate proteoglycan produced after spinal cord injury and is expressed by macrophages and oligodendrocyte progenitors. J. Neurosci., *22:* 2792–2803, 2002.

53. Chiang, C. S., McBride, W. H., and Withers, H. R. Radiation-induced astrocytic and microglial responses in mouse brain. Radiother. Oncol., *29:* 60–68, 1993.

54. Hong, J. H., Chiang, C. S., Campbell, I. L., Sun, J. R., Withers, H. R., and McBride, W. H. Induction of acute phase gene expression by brain irradiation. Int. J. Radiat. Oncol. Biol. Phys., *33:* 619–626, 1995.

55. Daigle, J. L., Hong, J. H., Chiang, C. S., and McBride, W. H. The role of tumor necrosis factor signaling pathways in the response of murine brain to irradiation. Cancer Res., *61:* 8859–8865, 2001.

56. Vallieres, L., Campbell, I. L., Gage, F. H., and Sawchenko, P. E. Reduced hippocampal neurogenesis in adult transgenic mice with chronic astrocytic production of interleukin-6. J. Neurosci., *22:* 486–492, 2002.

57. Seri, B., Garcia-Verdugo, J. M., McEwen, B. S., and Alvarez-Buylla, A. Astrocytes give rise to new neurons in the adult mammalian hippocampus. J. Neurosci., *21:* 7153–7160, 2001.

58. van Praag, H., Kempermann, G., and Gage, F. H. Running increases cell proliferation and neurogenesis in the adult mouse dentate gyrus. Nature Neurosci., *2:* 266–270, 1999.

59. Palmer, T. D., Markakis, E. A., Willhoite, A. R., Safar, F., and Gage, F. H. Fibroblast growth factor-2 activates a latent neurogenic program in neural stem cells from diverse regions of the adult CNS. J. Neurosci., *19:* 8487–8497, 1999.

60. Kuhn, H. G., Winkler, J., Kempermann, G., Thal, L. J., and Gage, F. H. Epidermal growth factor and fibroblast growth factor-2 have different effects on neural progenitors in the adult rat brain. J. Neurosci., *17:* 5820–5829, 1997.

176. THE EFFECT OF HYDROCEPHALUS ON IQ PRIOR TO FOCAL IRRADIATION IN CHILDREN WITH LOCALIZED EPENDYMOMA

Thomas E. Merchant, Heather Lee, Junhong Zhu, Xiaoping Xiong, Gregory Wheeler, and Raymond K. Mulhern. St. Jude Children's Research Hospital, Memphis, TN

To determine the influence of hydrocephalus, as determined by ventricular dimensions, on pre-irradiation IQ in children with local-ized, infratentorial ependymoma. Two classical measurements of ventriculomegaly, the Evans index and the cella media index, were performed on MR imaging studies obtained at the time of diagnosis and up to 12 months after the initiation of radiation therapy in 59 children with localized, infratentorial ependymoma. The Evans index (EI) is the ratio of the distance between the most lateral aspects of the anterior horns of the lateral ventricles and the maxi-mum lateral diameter of the cerebrum. The cella media index (CMI) is the ratio of the distance between the outer aspects of the lateral ventricles in the cella media and the lateral diameter of the skull in the parietal region. The study included 29 female and 30 male patients with a median age of 2.6 years (range 1.1-22.9 years) at the time of irradiation. Fifty (85%) had a clinical diagnosis of hydro-cephalus and 23 (39%) required CSF shunting. The extent of resec-tion was classified as gross or near-total in 50 (85%). Pre-irradiation IQ was measured using age- appropriate testing. The correlation between ventricular indexes and pre-irradiation IQ was investigated using a standard regression technique using index measurements from the time of diagnosis, and serial index measurements modeled from the time of diagnosis and up to one year after irradiation. For the serial measurements, a linear expression was used for each patient and the resultant intercept and slope were used as variables in the final model. IQ was considered the primary response variable. A generalized linear model was used that included important clinical variables. There was a strong correlation between EI and CMI (p<0.0001). The indexes obtained at the time of diagnosis predicted baseline IQ with higher EI and CMI values associated with lower IQ scores (p=0.0088). When serial measurements were modeled as a function of time, pre-irradiation IQ was found to be significantly influenced by EI and CMI obtained at the time of diagnosis (inter-cept) (p<0.05) and by the presence of CSF shunting when combined with the intercept value (p<0.05). Patients with higher index meas-urements and CSF shunting had lower scores. The rate of change in EI or CMI did not significantly influence pre-irradiation IQ. The resulting linear regression model for the IE index is: IQ pre-irradia-tion = 103.51 - 49.89 x (baseline EI) -35.07 x (baseline EI) x (shunt), where shunt is classified according to presence (value = 1) or absence (value=0). The study patients were characterized by an EI of 0.31 ± 0.11 (range 0.20 – 0.91) and CMI of 0.34 ± 0.10 (0.04 – 0.62) at the time of diagnosis (median ± SD). IQ scores were 89.50 ± 17.86 (range 50.0 – 132.0) prior to irradiation. IQ measured prior to irra-diation is significantly influenced by the extent of hydrocephalus at diagnosis. Hydrocephalus is an important clinical factor to include in the analysis of the effects of therapy. Additional analyses are required to determine its long-term effects.

177. PRELIMINARY TOXICITY REPORT ON RTOG 9803, A PROSPECTIVE DOSE ESCALATION TRIAL USING 3D CONFORMAL RADIATION THERAPY (3DCRT) IN GLIOBLASTOMA MULTIFORME

Jeff Michalski, Kathryn Winter, Matthew Arquette, James Purdy, David Brachman, Walter Curran, Joseph Simpson, and Minesh Mehta. Washington University, St. Louis, MO (J.M., M.A., J.S.); Radiation Therapy Oncology Group, Philadelphia, PA (K.W.); Image-Guided Therapy Center, St. Louis, MO (J.P.); Foundation for Cancer Research, Phoenix, AZ (D.B.); Thomas Jefferson University, Philadelphia, PA (W.C.); University of Wisconsin, Madison, WI (M.M.)

The RTOG is conducting a radiation dose escalation trial of 3-DCRT in patients with newly-diagnosed glioblastoma multiforme (GBM). This report describes acute and late toxicity on the first two dose levels of this trial (66Gy or 72Gy in 2Gy daily fractions). The study was designed not to allow excessive irreversible CNS toxicity compared to the RTOG historical experience. 104 patients were reg-istered and 100 eligible patients have received protocol therapy; 44 to 66Gy and 56 to 72Gy. Each patient was treated with 3D CRT to an initial clinical target volume defined by the resection cavity, resid-ual gross tumor and a margin of 1.5 cm and 0.3cm for setup error (PTV1). The resection cavity, residual gross tumor volume plus 0.3cm (PTV2) was boosted to a total 66Gy or 72Gy. Patients were stratified according to their boost planning target volume (PTV2 < or [2] 75cc). All patients received BCNU in addition to radiation ther-apy. Median followup is 10 months after 66Gy and 7 months after 72Gy. 14 patients at 66Gy and 10 patients at 72Gy experienced grade 3+ acute (<90days after start of RT + BCNU) non-hematologic toxicities. None of the acute neurological toxicities could be directly attributed to the radiation dose escalation. Another 5 patients expe-rienced grade 3+ non-hematologic BCNU toxicity following RT, including one BCNU related pulmonary death. There were only 3 occurrences of grade 3+ late RT toxicity. Two patients developed grade 3 brain toxicity after 66Gy and one patient developed grade 4 brain toxicity after 72Gy. This preliminary analysis reveals that excessive acute and late radiation toxicity has not been encountered with 3DCRT administered to doses up to 72Gy in 2Gy fractions. The 78Gy dose level is currently being tested. This work was supported by grant number RTOG U10 CA21661, CCOP U10 CA37422, Stat U10 CA32115) from the National Cancer Institute. Its contents are solely the responsibility of the authors and do not necessarily repre-sent the official views of the National Cancer Institute.

178. NEURAL PRECURSOR CELLS ARE EXTREMELY SENSITIVE TO IONIZING IRRADIATION

S. Mizumatsu[1], D. Morhardt[1], R. Rola[1], M.L. Monje[2], T.D. Palmer[2], and J.R. Fike[1]. [1]Brain Tumor Research Center, Department of Neurological Surgery, University of California, San Francisco, CA; and [2]Department of Neurosurgery, Stanford University, Stanford, CA

Therapeutic irradiation is commonly used in the treatment of brain tumors but can result in significant injury to normal brain structures. Severe tissue damage generally occurs after relatively high radiation doses, but less severe morphologic injury can also occur which has been associated with cognitive impairment. Radia-tion-induced cognitive changes may involve the hippocampus, but the pathogenesis of such injury is not well understood. We addressed acute hippocampal radiation response in male and female C57BL mice by exposing them to whole brain irradiation (0.5 -15 Gy) and quantifying cell responses using immunohistochemistry. Apoptotic cells (TUNEL), proliferating cells (Ki67) and immature neurons (Doublecortin) were quantified in the subgranular zone (SGZ) as a function of time and dose. In addition, neurogenesis (proliferation, migration and differentiation) was assessed 2 months after doses of 0, 2, 5 and 10 Gy. The dose response for SGZ apoptosis was deter-mined 12 hr after irradiation and was characterized by an extremely steep dose response from 0-2 Gy and a plateau from 2-15 Gy; females appeared slightly less sensitive after lower doses. Proliferat-ing cells and immature neurons were the most sensitive cells, and 48 hrs after irradiation they were reduced by 96 ± 3.5% and 78 ± 1.4%, respectively, relative to controls. SGZ proliferation was still reduced 2 months following irradiation, and in irradiated mice fewer BrdU-positive cells expressed the neuronal marker NeuN. These results show that proliferating SGZ cells and immature neurons are very sensitive to irradiation, and that acute cell loss is manifest at later times as reduced proliferation and neurogenesis. The functional con-sequences of such changes need to be determined but it is possible that prolonged changes in SGZ proliferation and neurogenesis may play a key role in radiation-induced cognitive dysfunction. Sup-ported in part by NIH R21 NS40088 and DAMD17-01-1-0820.

179. RADIOSENSITIZATION OF HUMAN MALIGNANT GLIOMA BY THE SIGNALING INHIBITOR LY294002

J.L. Nakamura, N.D. Arvold, and D.A. Haas-Kogan. Department of Radiation Oncology, University of California, San Francisco, CA

The phosphoinositide 3-kinase (PI3-kinase) signaling pathway is frequently activated in glioblastoma multiforme (GM) by mutation or loss of the 3' phospholipid phosphatase PTEN. Recent studies indicate that PI3-kinase activation increases resistance to radiation induced cell death, and PI3-kinase inhibition can radiosensitize var-ious tumors. While this has not been confirmed in glioma, GM radioresistance may be a consequence of PTEN loss and PI3-kinase activation. We sought to determine whether PI3-kinase inhibition would radiosensitize GM cell lines and to identify signaling effectors that mediate such radiosensitization. The effects of LY294002, an inhibitor of PI3-kinase, on the toxicity of radiation were examined in two malignant glioma cell lines with known PTEN mutations: U87 MG and U251 MG. After treatment with LY294002 one hour prior to irradiation and every 24 hours thereafter, cells were irradiated with single doses ranging from 1-6 Gy. Cell proliferation was assessed using MTS assays. The effects of LY294002 with and with-

VOL 4 ISSUE 4

Workshop W01: Regenerative Responses of Neural Stem Cells to Injury and Disease

W01-01

New oligodendrocytes are generated after neonatal hypoxic-ischemic brain injury in rodents

A. U. Zaidi, D. A. Bessert, H. Xu, J. D. E. Barks, F. S. Silverstein and R. P. Skoff

Department of Anatomy and Cell Biology, Wayne State University School of Medicine, Detroit, MI and Departments of Neurology and Pediatrics, Univeristy of Michigan School of Medicine, Ann Arbor, MI, USA

Neonatal hypoxic-ischemic (HI) white matter injury is a major contributor to chronic neurological dysfunction. In a P7 neonatal rodent stroke model, we studied oligodendrogenesis after HI injury. P35 control and HI-injured rats received multiple BrdU injections from either P12–14 or P21–P22. P35 brain sections were double-labeled for BrdU and glial markers for OLs [carbonic anhydrase-II (CA-II)], astrocytes [glial fibrillary acidic protein (GFAP)] and microglia (ED-1). In the injured corpus callosum and striatum, the number of BrdU+ cells is consistently greater than controls. At P35, generation of new astrocytes is seen in the gliotic infarct core and a microglial response is evident on the injured side. Significantly more CA-II+/BrdU+ cells are observed in the injured striatum, cingulum, corpus callosum and, surprisingly, in the infarct core. These results indicate the neonatal brain retains the potential to generate new OLs up to 4 weeks after an HI injury, at levels significantly above their normal rate of production.

W01-02

Recruitment of neural stem cells following perinatal hypoxic/ischemic insult

S. W. Levison, M. J. Romanko, R. P. Rothstein and M. J. Snyder

Neuroscience and Anatomy, Penn State College of Medicine, Hershey, PA, USA

Babies born prematurely frequently experience episodes of hypoxia and ischemia (H/I) which can permanently damage the brain. As neural precursors are abundant and generate new brain cells during this period, we have been studying the vulnerability and responses of neural stem cells and progenitors to perinatal H/I. Approximately 25% of the total cells in the subventricular zone (SVZ) die as a result of a moderate to severe H/I episode. The majority of the dying cells are located in the most lateral tip of the SVZ, which is a region that is enriched in progenitors. By contrast, cells in the more medial aspect of the SVZ, which is where the neural stem cells reside, sustain little permanent damage. At 2 days of recovery, the mitotic activity of the medial SVZ cells was increased as assessed by BrdU incorporation and PCNA staining. Additionally, the numbers of both PCNA/Nestin$^+$ and PCNA/GFAP$^+$ cells was increased. Furthermore, primary and secondary neurosphere assays revealed an approximate doubling in the number of stem cells in the damaged hemisphere vs. controls. This was corroborated by a significant increase in the percentage of the spheres that were multipotential. These data indicate that neural stem cells proliferate in response to a hypoxic/ischemic insult. We conclude that neural progenitors are vulnerable to perinatal H/I, whereas neural stem cells are not only resistant, but that they transiently increase in abundance. These data demonstrate that compensatory responses are initiated by neural stem cells in response to brain damage, which if appropriately harnessed and extended could provide the means to regenerate brain cells after perinatal injury.

W01-03

Proliferation and migration of subventricular zone cells in intact adult mice and after cortical lesions

F. G. Szele, G. E. Goings and H. K. Chin

Department of Pediatrics, North-western University, Chicago, IL, USA

Cells in the adult subventricular zone divide and give rise to young neurons which migrate rostrally to the olfactory bulbs. Injury to the adult brain increases SVZ cell numbers and induces a periventricular radial glial phenotype. We hypothesized that the total number of cells and the number of cells in S-phase would increase in the adult mouse SVZ after unilateral lesions of the cerebral cortex. We also hypothesized that SVZ cells would migrate into, and that radial glia-like cells would appear in adjacent structures such as the striatum. In contrast to what we have previously shown in rat, we found no changes in total cell numbers, but biphasic decreases in the numbers of cells in S-phase in mouse. We also demonstrated that in intact adult mice, retroviraly infected cells could migrate from the SVZ not only to the olfactory bulbs but also into the periventricular striatum, septum, and corpus callosum. This pattern of migration was confirmed in the same extra-SVZ regions by the expression of doublecortin, in cells with migratory morphology. Migration out of the SVZ was especially robust in the ventral-most areas of the lateral ventricle. The majority of the periventricular region was devoid of radial glia-like cells in intact mice and cortical lesions did not change this pattern, however, we found a population of vimentin and GFAP-positive radial glia-like cells at the base of the lateral ventricles. Our results demonstrate that there are interspecies differences in the regulation of SVZ cell numbers after injury. They also suggest that a small number of SVZ cells can migrate to non-olfactory bulb areas, even without brain injury. Finally, we propose that the ventral-most SVZ contains specialized cells that may serve as a substrate for migration.

W01-04

Ionizing radiation causes long-term inhibition of neurogenesis in the dentate gyrus

J. R. Fike, S. Mizumatsu, D. Morhardt, R. Rola and J. Raber

Brain Tumor Research Center, Department of Neurological Surgery, UCSF, San Francisco, CA 94143 and Department of Behavioral Neuroscience/Neurology, OHSU, Portland, OR, USA

Therapeutic irradiation involving the brain can result in significant injury to normal brain structures. Although severe tissue damage generally occurs after relatively high radiation doses, less severe injury can also occur which can lead to cognitive impairment. While the pathogenesis of such injury is not well understood, it may involve neural stem/precursor cells in the dentate subgranular zone (SGZ). The SGZ is extremely sensitive to therapeutically relevant doses (2–10 Gy) of X-rays, and significant dose-dependent decreases in the numbers of proliferating cells and immature neurons are observed 12–48 h after irradiation. Cell proliferation is still reduced months after irradiation and neurogenesis is substantially affected. While there are no apparent changes in production of new astrocytes, there is a dose-dependent decrease in the production of new neurons and a slight increase in the number of new oligodendrocytes. While the mechanism behind these changes in neurogenesis is not yet clear, it may involve environmental factors including local inflammation and changes in the microvasculature. Recent data show that after an X-ray dose that significantly affects the birth of new neurons, there is a concomitant reduction in hippocampal-dependent cognitive function. These results show that X-irradiation substantially alters neurogenesis in the dentate SGZ, and suggests that such changes may play a contributory if not casual role in radiation-induced cognitive impairment.